GRAPH THEORETICAL ANALYSIS OF FUNCTIONAL HUMAN BRAIN NETWORK

by

Adem Umut Günebakan

B.S. in Electronics Engineering, Işık University, 2008

Submitted to the Institute of Biomedical Engineering
in partial fulfillment of the requirements
for the degree of
Master of Science
in
Biomedical Engineering

Boğaziçi University
2011

ACKNOWLEDGMENTS

First of all, I would like to thank to my thesis advisor, Prof. Dr. Ahmet Ademoğlu, for his academic support and friendly supervision. I am deeply grateful to my co-advisor, Assist. Prof. Dr. Rifat Koray Çiftçi, for his guidance, support and suggestions. I am also grateful to TUBITAK for fundings of this study (Project Number: 109E202).

I feel grateful Assoc. Prof. Dr. Ata Akın who aided us during our experiments and opened the door of Biomedical Optical Imaging and Sensors Laboratory for our experiments. Also, I see myself obliged to Namık Kemal Univesity Biomedical Engineering Laboratory, my second home, for its comfortable and high-tech environment during analysis of this study.

I am indebted to Prof. Dr. Yorgo Istefanopulos and to Assist. Prof. Dr. Hakan Gürkan for leading me to neuroscience studies.

Besides academic people, I feel grateful to Çağatay Aydın for his great supports since my undergraduate studies; Oytun Oktay, for his short time accommodation support in Çorlu; Barış Bulutlu, for his sincere behavior; İsmail Devecioğlu, for his dorm friendship; Sinem Burcu Erdoğan, for her great charity; Esin Karahan, for her serious conversations on neuroscience; Zeynep Susam and her fellows, for remaining motivation and encouragements; participants, for their great patience during experiment.

Lastly, I want to thank my father, Mustafa Suat Günebakan, and mother, Necla Sarsmaz. They have brought up me to these days with love and confidence.

ABSTRACT

GRAPH THEORETICAL ANALYSIS OF FUNCTIONAL HUMAN BRAIN NETWORK

Recent studies suggest that, human brain has a small-world behavior which is reflected by locally and globally efficient processing. To investigate this behavior a short term/working memory experiment was designed which had manipulation and retention conditions. Our goal was to be able to explore the differences between the organizations of the brain during the execution of these tasks within a graph theoretical context. The retention condition required the subject only to remember a visually applied stimulus whereas the manipulation condition to visually manipulate the stimulus before keeping it in mind. Brain activity information was recorded through the electroencephalography (EEG) device. After preprocessing, the collected EEG data was decomposed into classical frequency bands and phase locking values (PLV) between each pair of electrodes were computed with the help of the Hilbert Transform. After applying thresold to PLV matrices to build binary unweighted networks, the graph theoretical analysis was applied to determine and compare the main dynamics of functional coupling during manipulation and retention. This analysis was carried out in a time dependent manner to better monitor the variations of these dynamics. It was found that the brain exhibited a highly efficient behavior in the local and global sense both during manipulation and retention; and thus the brain had a small-world characteristic during the execution of these tasks. The statistical analysis revealed significant differences between the efficiency values of retention and manipulation. The analysis of node and edge centrality values of different frequency bands showed prominent effects in the upper alpha gamma bands. The finding of this thesis study supports the feasibility of the graph theoretical analysis for analyzing complex brain networks.

Keywords: Synchronization, Betweenness Centrality, EEG, Working Memory, Global Efficiency, Local Efficiency, Small-World, Graph Theory

ÖZET

İŞLEVSEL İNSAN BEYİN AĞLARININ ÇİZGE KURAMI İLE İNCELENMESİ

Son çalışmalar, insan beyninin küçük dünya davranışı sergilediğini ve bunun yerel ve bütüncül açıdan verimli bilgi işleme süreci yansıttığını ortaya koymaktadır. Bu davranışı incelemek için hileli akılda tutma ve doğrudan akılda tutma durumlarının bulunduğu, kısa süreli/işlek bellek deneyi tasarlanmıştır. Hedefimiz beynin düzeninin farklılıklarını görevler yerine getirilirken çizge kuramı bağlamında incelemektir. Denek, akılda tutma durumunu sadece görsel uyaranı hatırlayarak; hileli akılda tutma durumunu ise görsel uyaranı değiştirdikten sonra akılda tutarak gerçekleştirecektir. Beyin faaliyet bilgisi elektroensepalogram (EEG) cihazı ile kaydedilmiştir. Toplanan EEG verisi önişledikten sonra tipik frekans bantlarına ayrılmış ve her çift elektrod için Hilbert dönüşümü sayesinde faz kilit değerleri (FKD) hesaplanmıştır. Çift değerli ağırlıksız ağ oluşturmak için FKD matrisleri eşiklendikten sonra, akılda tutma ve hileli akılda tutma durumları sırasındaki işlevsel bağlantı ana dinamiklerini belirlemek ve kıyaslamak için çizge kuramı analizi uygulanmıştır. Dinamiklerin değişimlerini gözlemlemek için zamana bağımlı bir tutumda bu analiz hayata geçirilmiştir. Akılda tutma ve hileli akılda tutma durumlarında beynin yüksek seviyede yerel ve bütüncül anlamda verimlilik sergilediği; böylece beynin bu durumları yürütürken 'küçük dünya' karakterine sahip olduğu bulunmuştur. İstatistiksel analiz, akılda tutma ve hileli akılda tutma durumları için verimlilik değerlerindeki kayda değer farklılıkları ortaya çıkarmıştır. Değişik frekans bantlarındaki uç ve kenar merkeziyetçilik değerleri, alfa ve gama bandında göze çarpan etkileri göstermiştir. Bu tez çalışmasındaki bulgular, çizge kuramı analyizinin karmaşık beyin ağlarında uygulanabiliriğini desteklemektedir.

Keywords: Eşzamanlama, Ara Merkeziyetçilik, EEG,İşlek Bellek, Bütüncül Verimlilik, Yerel Verimlilik, Küçük Dünya, Çizge Kuramı

TABLE OF CONTENTS

LIST OF FIGURES

LIST OF TABLES

LIST OF SYMBOLS

G	Graph
E	Number of edges
V	Number of vertices
$a_{i,j}$	Relation value between node i and j
ϕ	Phase value
k_i	Degree of node i
i	Vertex number
e_i	Existing edges of node i
$d_{i,j}$	Distance between node i and j
E_{Global}	Global Efficiency
E_{Local}	Local Efficiency
C	Average Clustering Coefficient
L	Average Path Length
b_i	Betweenness Centrality
$n_{j,k}(i)$	Shortest paths between j and k that run through i
α	Description of α

LIST OF ABBREVIATIONS

EEG	Electroencephalography
PLV	Phase Locking Value
WM	Working Memory
fMRI	Functional Magnetic Resonance Imaging
MEG	Magnetoencephalography
PET	Positron Emission Tomography
STM	Short Term Memory
CNS	Central Nervous System
ERP	Event Related Potentials
CC	Cycle Criterion
FIR	Finite Impulse Response
FDR	False Discovery Rate

1. INTRODUCTION

1.1 General Background

Electroencephalography (EEG) is the measurement of electrical activity on scalp that generated from the neurons in the brain [1]. Hans Berger first discovered electrical activity on the scalp was alpha rhythm (8-12 Hz) in 1875 and then Caton advanced his discovery on animal subjects in 19th century [2, 3]. Electrical activity patterns of brain obtained from the EEG are described with the help of the electrodes in millivolts degree in the form of oscillating signals.

Significant EEG oscillations are decomposed not only by their frequency also by their phases. For a working memory (WM) task, presentation of stimuli forms the initialization of the phase of theta band (4-7 Hz) in the hippocampus (Figure 1.1) [4, 5]. Therefore, besides frequency components, phase information is significant [6]. By using EEG oscillations; connectivity of brain can be determined in terms of phase and frequency.

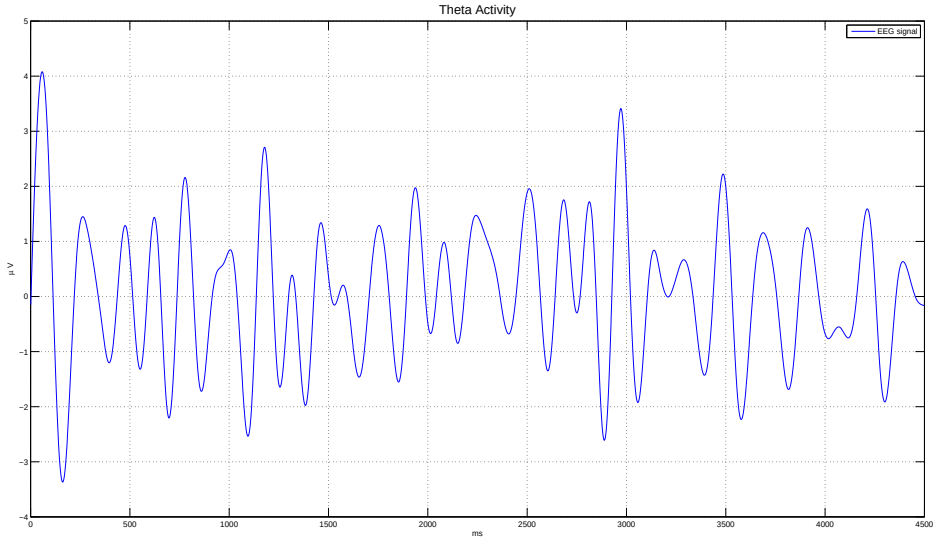

Figure 1.1 Theta Activity of human brain (4-7 Hz).

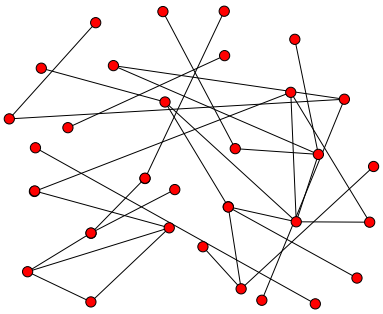

Figure 1.2 Graph Example

Brain connectivity is defined in terms of structural, effective and functional connectivities. Structural connectivity refers to network of anatomical links which are the layout of axons and synaptic connections. Structural connection investigates the neuronal neighborhood relationships within a predetermined region of interest. Effective connectivity denotes directed or causal relations of system elements in the brain. Functional connectivity is the statistical dependency or association between elements of a system using the time series measured from these regions [7, 8]. Focusing on neurophysiological modalities, fMRI (Functional Magnetic Resonance Imaging) has high spatial resolution then that of EEG. However, EEG has more detailed temporal resolution than fMRI. When we study functional connectivity, statistical metrics between time series collected from interrelated regions give us valuable information about the degree of connectivity [9]. Because brain has a complex structure, graph theoretical approaches are suitable for representation of such a complex network [8].

Graph theory was first pioneered by Amaral and Ottino [10] and the first work was demonstrated with the nervous system of a nematode with 282 neurons [11]. Functional connectivity of brain was represented by graph theoretical model in some brain studies [7]. By using this model, various brain analyses have been done with healthy and/or diseased brains [12, 13, 14].

Sprons has investigated the neural structure in terms of functional and anatomical connectivity using graph theoretic approaches [15, 16]. The dynamical modeling

of the brain using graph theoretic approaches allow us investigating higher brain processes such as memory, planning, visual or sensual response and various types of brain pathophysiology by using different decompositions.

1.2 Motivation

The electrical activity of brain has been studying for decades with invasive and non-invasive imaging modalities. Usage of invasive imaging modalities are hard to implement to subjects, whereas non-invasive modalities are easier than invasive ones. Investigation or diagnosis of healthy or diseased brain is more practical with non-invasive modalities. Importance of these modalities are also changing by their area of usage.

While investigating functional connectivity of the brain, modalities such as fMRI, EEG, MEG, PET modalities can be used. Connectivity can be analyzed with different methods. When dealing with functional connectivity which changes over time, better time resolution is needed. In terms of complexity and cost EEG can be the most suitable modality for investigation of functional connectivity.

Many methods and techniques have been used for investigation of functional connectivity. In recent years, graph theoretical approach is getting more popular because brain has a network structure like other complex networks in nature.

However, many problems occur on examination of functional brain networks. Every researcher generates a certain graph and there is no transition among different graph structures. Moreover, the choices of parameters in the models have a great effect on results [17, 18] such as threshold or graph construction. Clusters of these experiment groups can be different.

The motivation of this thesis study is defined as to understand, compare and facilitate different network structures that yield easily computable measures which

characterize the functional brain network topology. New methods on different networks studied. Different threshold levels investigated that are subjected to a cognitive task. Synchrony of oscillations among different bands investigated with respect to frequency dependent time windows.

1.3 Objectives

In this study, we investigate the graph theoretical analysis of functional human brain networks. For this purpose, manipulation and retention tasks implemented to the subjects to examine the EEG synchrony measures. After that, Hilbert transform used for generating complex components of the various EEG bands in MATLAB environment. Phase information calculated from the trigonometric measures of real and imaginary parts of the signal. Phase Locking Values (PLV) obtained with the help of the phase differences of all pairwise EEG electrodes with respect to the time series of specific frequency bands. By using a frequency dependent time-window method used that is based on slowest oscillation limit of each frequency band. Adjacency matrices obtained with PLV measures. Specific threshold levels used for determining binary matrices from weighted ones. Graph theory metrics are calculated and statistical analyses are done.

Efficiencies of the graphs will be calculated and changes over time windows with different thresholds are revealed. Significant nodes and edges will be visualized over a head model of centrality measures ($p < 0.05$). Significant manipulation and retention efficiency values of subjects will be statistically analyzed. Determination of false detection rate masks computation will be done to statistical evidences to gather more accurate results.

1.4 Outline of this thesis

The remaining chapters are organized as follows. Chapter 2 gives a brief outline of EEG and their oscillations. Interactions between psychological tasks and functional connectivity of brain is discussed, thus electrical activity on graph theory is explained in detail. Creating a graph by use of a Phase Locking Value (PLV) is explained and the chapter concludes with a brief background on how functional connectivity can be estimated via graph theory. A detailed explanation of the methods is given in Chapter 3 where preprocessing operations such as filtering, artifact removals and analyses of EEG data to obtain a graph are discussed. In Chapters 4,5 and 6; results, discussion and conclusion are defined respectively.

2. Electro-physiological Oscillations of Functional Connectivity via Graph Theory

2.1 Graph Theory

Up to the mid-eighteenth century, people believed that it was impossible to cross over the bridges of the river Pregel at once and returning to the start point in the city of Königsberg (Figure 2.1). But in 1736, Euler suggests a mathematical method to traverse these seven bridges where located on the river Pregel and he represented this method with a graph and it was called as graph theory [19]. After this problem Fancis Guthrie comes up with a problem which is called the four color problem. This problem suggest that making a world map where all countries are colored with one of four colors and neighbor countries must not have same colors. Surprisingly, this problem took 124 years to solve, from 1852 to 1976 with the invention of computers and their improvements [20]. Also in 1959, Erdős and Rényi suggested the random graph model which has the same node and degree distribution of that of regular graph. Random graphs allow modeling of complex graphs with newly graph metrics [21].The most complex networks are modeled with the "small-world phenomenon". This phenomenon was first introduced as "The Small World Problem" for social networks with Stanley Milgram in 1967 [22]. All nodes of small-world networks are not neighbors to each other yet it is possible to travel one to another node by visiting the other nodes [23]. The most remarkable property of these networks is that the clustering coefficient is high as regular networks and path length are low as random networks. This type of networks can be a bridge between random and regular networks. Watts and Strogatz also mentioned that in nature most of the networks showed small-world property such as genetic networks, spatial games, excitable media, social issues and neural networks. Nowadays, social networks is the significant example for this theory which are proving that even very large networks can be traversed. These improvements in the technology are now resulting with the implementation of the graph theory in biology and neuroscience. Neural systems are good examples which have long been described as sets of

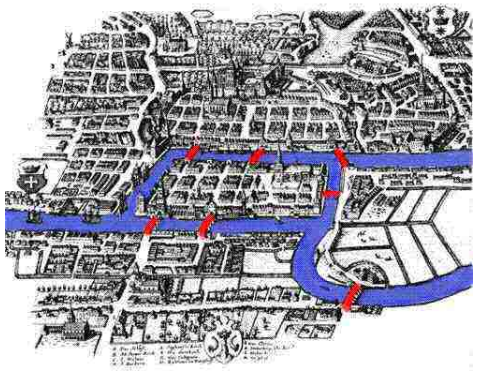

Figure 2.1 Bridges of Könisberg

discrete elements linked by connections. [8]. As a neural system, human brain is taken into account as a complex network [24]. Functional [11] and structural [23] connectivity are represented by the graph theory in many studies in humans [25, 26] and in animals [23, 27].

Major brain imaging modalities such as fMRI, EEG and MEG (Magnetoencephalography) have been used for analyzing the connectivity of brain. Graph theoretical implementation of brain via fMRI was first measured in human brain at resting state [28]. Metrics of networks approximated from voxel based graphs. Many studies ensued after this study in [29, 30, 31]. When we focus on electrophysiological imaging modalities, we have a higher temporal resolution than that of MRI. However, using MRI, we can get more detailed spatial resolution compared with that of the EEG/MEG. fMRI based networks are derived from anatomically localized regions of the image.

Furthermore, functional connectivity is better approximated by electrophysiological modalities such as EEG, MEG with generalized synchronization [8]. Measurements of functional connectivity are studied in healthy [32] and diseased subjects [12, 13, 14]. Diseases such as Alzheimer's, schizophrenia or epilepsy caused disconnectivity between regions.

In recent years, challenging cognitive processes topics are also studied with graph theory via synchronization, correlation and coherence over neuronal oscillations.

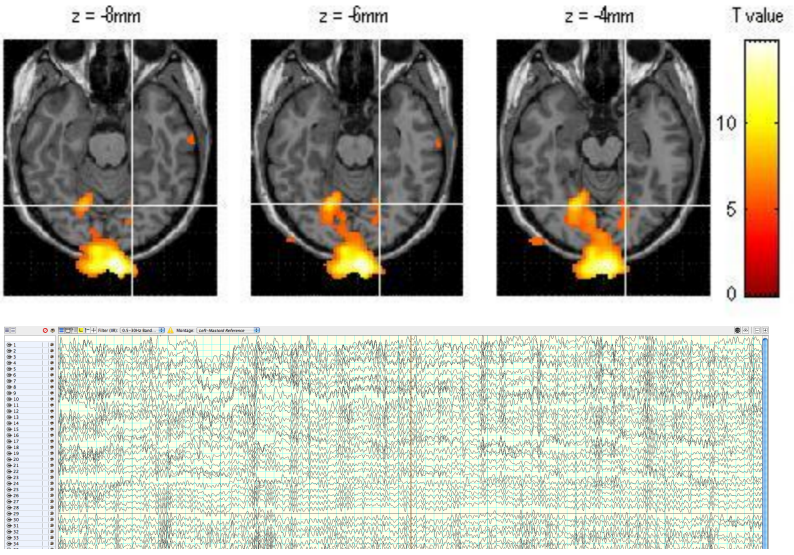

Figure 2.2 fMRI and EEG recordings.

2.2 EEG

Brain has a complex structure where nerve and glial cells are in interaction. Human central nervous system (CNS) contains 10^{11} neurons. Number of glial cells is approximately 10-50 times more than nerve cells. CNS collects the data from various sense organs and yields for necessary response [33, 34]. This neuronal activity, the simplest evolution level to most complex human cerebral cortex level stands for electrochemical activity. Monitoring chemical activity of neurons is not an easy task, but electrical potential changes can be easily monitored by electroencephalogram. EEG signal that is generated from the synchronized post-synaptic potentials in cerebral cortex; can be monitored and recorded through the electrical potential differences from the scalp [35]. Electrodes which are placed on the scalp, record the EEG data. Because of the volumetric conduction, neurons under the scalp and far located neurons are generates the EEG signal. Postsynaptic potentials are more dominant to EEG oscillations [36, 37, 38].

2.2.1 EEG Oscillations

Neural brain signals oscillate across a range of frequencies with respect to their frequency spectrum. Firstly, band alpha which oscillates between 8-12 Hz, was first discovered in late nineteenth century [2]. Ever since that time, other frequency bands became clearer. Based on the brain functions, five more major frequency waves are discovered, delta wave (0-4 Hz), theta wave (4-8 Hz), alpha wave (8-12 Hz), beta wave (14-30Hz), gamma wave (>30Hz)(Figure 2.3) [39]. Brain oscillations are observed by using electrophysiological modalities such as EEG or MEG which records synchronous activity of various neurons except invasive imaging modalities. Neural activity analysis can be done by using amplitude, frequency and phase measures.

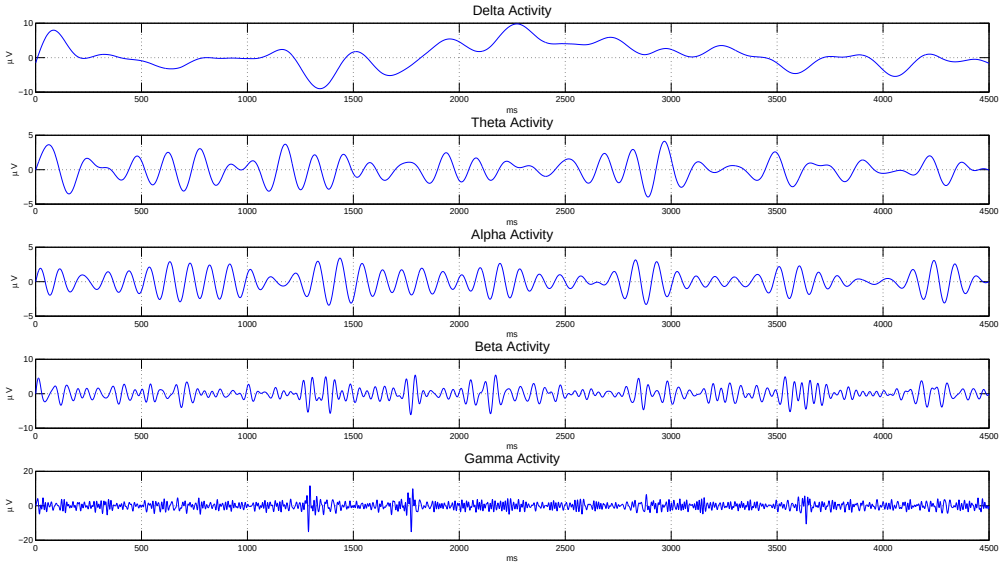

Figure 2.3 EEG bands.

A time-frequency analysis can be done for extracting necessary frequency specific information. Variations in frequency bands indicate various brain functions in humans. When a person is relaxed and drowsy alpha wave becomes more dominant. Beta waves are observed if a person is fully awake and alert. Creative thinking and mediation is correlated with theta waves. For deep and dreamless sleeping delta waves become more

dominant with their highest amplitude when comparing with other bands. Besides these permanent waves, there are transient waves are occuring on an EEG signal such as spikes, vertex waves, sleep spindles and sharp waves. Their identification is much more difficult than permanent waves because they come and go [39]. Transient waves are using for diagnosis of a specific brain disorder. For example, spikes and sharp waves can arise from epileptic seizures. Clinics are recording these brain data to predict epileptic regions of the brain. Because EEG is not as expensive as invasive imaging modalities, it is also used for monitoring anesthesia level, sleeping stage, strokes, comas or deathly brain disorders.

Changes in synchronization within a neural ensemble are resulted from amplitude changes of oscillatory signals. Synchronization is mostly related to the cognitive functions of the brain such as memory, attention or perception. Furthermore, synchronization metrics can be indicator of information transfer between neurons.

2.2.2 Graph Theory via EEG

For understanding the characteristics of a functional network of human brain, it is known that cognitive process such as memory and abstract reasoning is performed not only on a specific area but also by the interaction of numerous areas [40]. However, with the new studies due to the functional anatomy, the WM activity information can be observed in the medial temporal lobe and prefrontal cortex in a widespread manner. In addition, novelty detection related tasks, such as manipulation can be observed as a contribution of the hippocampal region to generate ERP (Event Related Potential) on scalp. In the light of this complexity in terms of EEG processing, graph theoretical approach should have a great role for describing functional network information of human brain.

Various metrics have been used in graph theoretical approached networks that should help to describe information flow of electrical activity of the brain in an efficient manner. Most of the frequently used metrics of graph theory are clustering

coefficient and path length. Clustering coefficient of the functional network should give contraction information of task related synchronized activation in different brain regions. In addition, the information flow on the functional network topology can be described with the help of path length measures. According to the previous studies brain networks have small-world characteristic similar to the other networks in nature [41, 24]. Due to the small-world property, brain networks have high clustering coefficients and low path length which correspond modular and integrated information processing respectively [41]. If the path between two nodes does not exist, the length is considered to be infinite. This indicates the efficiency of those pairwise nodes is zero. Furthermore, network information flow of the brain can be regarded as bilateral, global efficiency of the network is an easier tool for estimating parallel information transfer. The average efficiencies of whole pair wise nodes, gives us the global efficiency metric of the network. Thereby observing specific brain areas, they can be considered as sub graphs. Dealing with sub graphs, average efficiency of those is called average local efficiency of a network. To provide information for handling disconnected nodes, the efficiency metrics contain the information to solve a graph better than with clustering coefficients or path lengths [42].

Besides disconnected nodes, a graph can contain a node which can be described as a hub. Hubs have high degree or centrality. The centrality measures how many nodes are connected to a node. Because of this, high centrality provides efficient communication [43]. So, centrality determines notational importance of a nod in a graph. Therefore, *node betweenness centrality* is a measure of a node in terms of centrality. If a node has a high degree and is located on shortest paths of various nodes, it will have high node betweenness centrality measure. If a group is loosely connected by a few edges, shortest paths between different groups go through one of these few edges. The edges connecting groups will have high *edge betweenness centrality* value [44].

Application of graph theoretical approach to functional human brain network with EEG, an undirected binary graph must be derived from data by applying a threshold value to constructed graphs [45]. Recording the electrical oscillations from brain,

functional connectivity can be estimated between a pair of regions in terms of synchrony. Oscillations can be filtered to classical EEG bands to observe different characteristics of that time series and band definitions. According to Jacobs et al., theta oscillations are relevant to memory load, task difficulty and error processing. Also alpha power increases with memory load in simple WM tasks. In addition previous studies show that gamma power was correlated with memory load, attention and reaction time [18].

Consequently, brain is a complex network and supports compatible with modular or integrated processing since network character is based on senorimotor and cognitive processes. Brain network has the ability of minimum cost of information processing, maximum efficiency of parallel data processing and there are rare connectivity between regions with low wiring costs. Network is operating with gathered neuronal activity with variations of cognitive states [41].

3. METHODS

3.1 Experimental Procedure and Subjects

19 healthy right-handed subjects participated in this experiment (5 female, 14 male, mean age: 25.4±1.9). All of the participants volunteered and signed an informed consent about the experimental protocol. At the beginning of this visuospatial experiment, one minute baseline recording done at eyes open state. At this baseline recording, a plus signed ('+') cursor was shown. For the rest of the experiment; subjects were asked to perform a visuospatial WM task. Three targets were shown on a four by four matrix for 500 milliseconds. If the targets were green which is a retention task, subjects had to keep in memory the position of targets for 2500 milliseconds. If the targets were red, which is a manipulation task; subjects had to keep in memory the mirror image positions of the targets along to horizontal axis. At the end of the 2500 milliseconds time interval, three gray targets appeared on the screen and subjects had to report whether the targets were wrong or right with the help of right or left mouse buttons respectively in 1000 milliseconds.

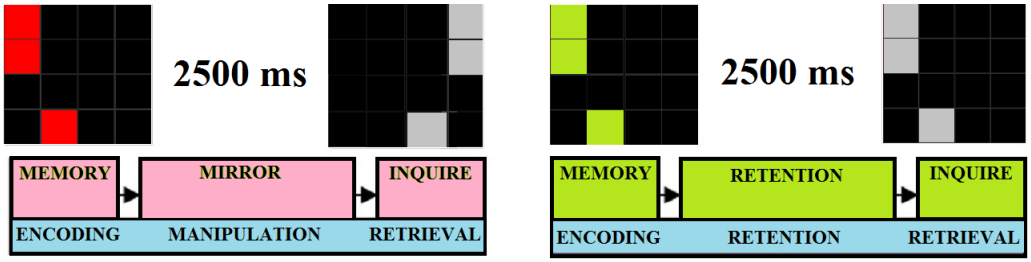

Figure 3.1 Experimental scheme.

Segmentations of 4500 milliseconds periods were done with 500 milliseconds before the first target was shown and 500 milliseconds after the gray targets were shown. Every stimuli and reaction events were recorded. Also, a log file was recorded which collects false and correct answers, stimuli time and type, average reaction time of correct answers, and minimum reaction time of a correct answer for both manipulation

and retention WM task for each subject [46, 47].

For the timing problem between presentation computer and recording computer, 2 milliseconds synchronization pulse was sent from presentation computer. After 4 stimuli, computers are synchronized at once.

There were 40 retention and 40 manipulation tasks. Equal number of false and correct trials were given for each task. Sequences of the trials were chosen randomly. All of the presentation trials were done by using the Psyctoolbox for Matlab.

3.2 Data Collecting

Recordings of the data were done with a EGI HydroCel 64 channel EEG instrument. Sampling frequency of recordings was 1KHz. Sponge electrodes were used. Chemical components of the conductive solution are water, potassium chloride (dry) and baby shampoo (non-alcoholic compound). At the preprocessing stage; raw data was filtered and removed from unwanted components. NetStation program was used at the preprocessing stage on a Macintosh computer.

3.3 Preprocessing

At the first stage of the preprocessing operation a first order FIR high-pass filter was used with 0.1 Hz cut-off frequency. After high-pass operation; filtered signal was passed through a 100 Hz low-pass FIR filter and then 50 Hz notch filter is used for getting rid of power line noise. With respect to the events which are marked on the raw data, segmentation was done for collecting correct manipulation and correcting retention data.

Artifact removal operation was applied for bad channels, eye blinks and eye

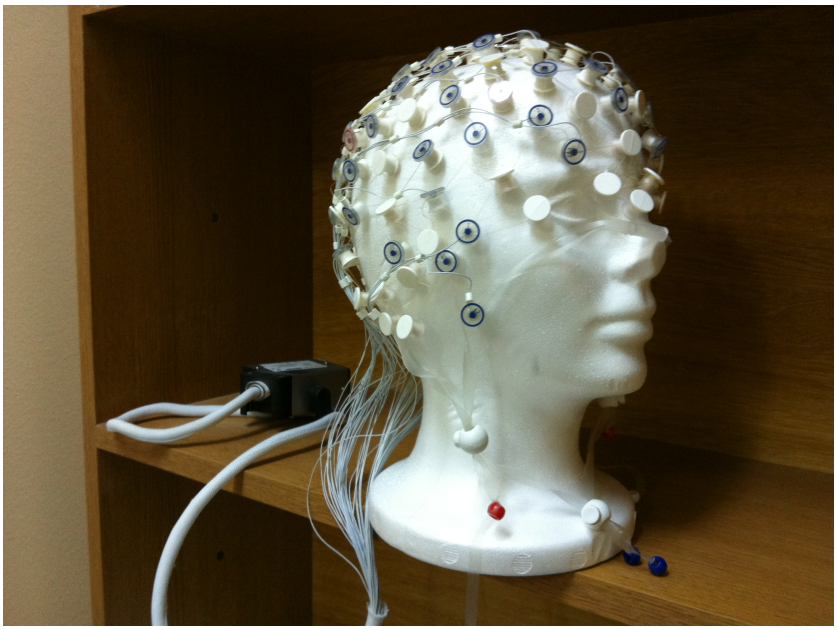

Figure 3.2 64 channel EEG cap with sponge electrodes.

movements over the entire time segment. Electrical potentials of channels which do not fall between ±200 μV with 80 milliseconds of duration are marked as Bad Channels. Eye Blink detection is done with ±140 μV boundaries for 640 milliseconds with a moving average window of 80 milliseconds duration. Signals which are not between ±55 μV for 80 milliseconds duration, are marked as Eye Movement artifacts. Artifact removal operations are done for any eye blink, eye movement and for more than 10 bad channels with a % 20 exception. NetStation's Ocular Artifact Removal (OAR) tool is used for to flatten eye blinked channels. Therefore, we can use more segments to have better results. Artifact Detection tool contains Eye Blink, Eye Movement and Bad Channel properties. Artifact detection and Bad Channel Replacement operations are done before and after OAR.

These segments are adjusted for suitable montage with montage operations and then exported to Matlab environment as '.mat' files.

3.4 Generating Functional Graphs

Once we discussed about the complexity of the human brain, graph theory is the main intermediary tool for analysis of functional connectivity. Since the functional brain network properties are estimated from electrophysiological imaging techniques, this can be analyzed via graph theory [32].

Vertices and edges: In graph theory, a graph contains edges and vertices. Vertices denote nodes and edges branches. An edge between two vertices is the sign of a connection of these vertices. A graph is represented by;

$$G(E, V)$$

where G denotes graph, E denotes edges and V denotes vertices.

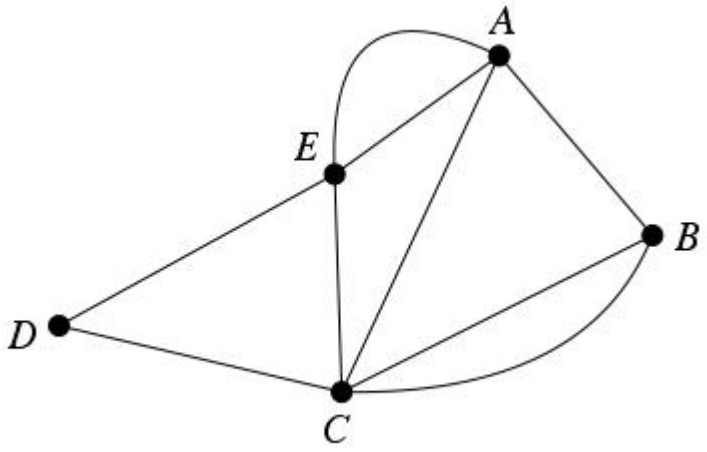

Figure 3.3 Graph with 5 vertices and 8 edges.

Adjacency matrix: Each edge value between two vertices is a connection indicator and can be shown in an adjacency matrix. This matrix has the communication information of all nodes ($a_{i,j}$) with each other [42]. Information can also connect with itself and a vertex can be connected to itself with an edge in classical graph theory.

$$\mathbf{X} = \begin{pmatrix} 1 & 0 & 1 & 0 & 0 \\ 1 & 0 & 1 & 1 & 0 \\ 0 & 0 & 1 & 0 & 1 \\ 0 & 0 & 1 & 1 & 0 \\ 1 & 0 & 1 & 1 & 0 \end{pmatrix}$$

Values of adjacency matrices can be binary (zeros or ones) and can be numerical values. Therefore they are called *binary* (unweighted) or *weighted* graphs, respectively. A weighted graph can be converted to a binary graph with a threshold value. Flowing information is not always two-sided and adjacency matrices are not always symmetrical. If the graph is not symmetrical, it can be called a *directed graph*. In a directed graph, information can only flow from one direction. However in a *undirected graph*, information flows in both directions.

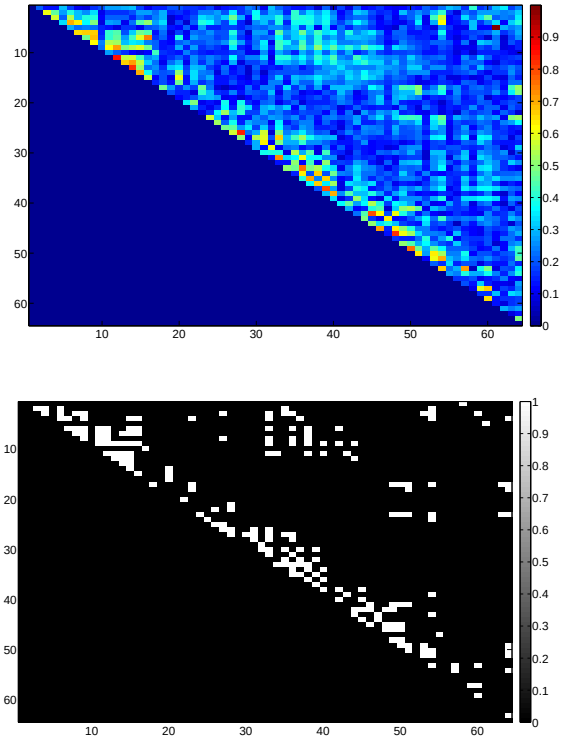

Figure 3.4 Weighted undirected adjacency matrix (top). Binary undirected adjacency matrix (bottom).

3.4.1 Band Specifications

At the analysis stage; there were only five frequency bands considered which are theta (4-8Hz), beta (13-30Hz), gamma (30-45Hz), lower alpha (8-10Hz) and upper alpha (10-12Hz). Least square FIR filters were used while decomposing the EEG data. Filter lengths were calculated by three times of sampling frequency over lower boundary frequency value of specific bands. Filters were linearly phased. Filtering operations are done in MATLAB environment.

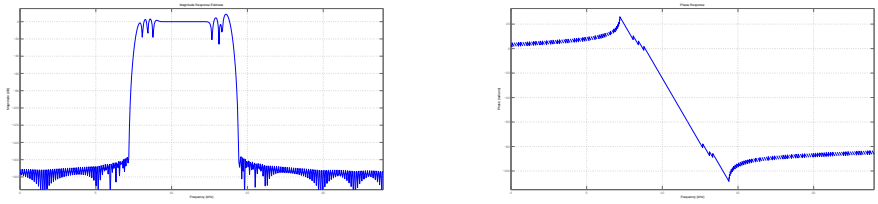

Figure 3.5 Magnitude and phase response estimation of the filter.

3.4.2 Hilbert Transform

For the calculation of phase values we need to decompose the signal into imaginary and real parts. Hilbert Transform is one of the specific transformation techniques that enable us to obtain these parts.[48].

Hilbert Transform's property is like Fourier Transform which provides relationship over phase and amplitude spectrum with real and imaginary values.

$$s(t) = s_i(t) + s_r(t) \tag{3.1}$$

We can define our $s(t)$ function with $s_r(t)$ and $s_i(t)$ which are real and imaginary respectively. If values of the functions are equal to zero for all t values, these functions will be even and odd functions.

$$s_r(t) = s_r(-t) \tag{3.2}$$

$$s_i(t) = -s_i(t) \tag{3.3}$$

With the constraints above;

$$s(t)_r = \frac{1}{2}[s(t) + s(-t)] \tag{3.4}$$

$$s(t)_i = \frac{1}{2}[s(t) - s(-t)] \tag{3.5}$$

these functions will be obtained. Frequency responses of these functions are defined below.

$$S_i(f) = -4\int_0^\infty \cos(2\pi ft)dt \int_0^\infty S_r(u)\sin(2\pi ut)du \tag{3.6}$$

$$S_r(f) = -4\int_0^\infty \sin(2\pi ft)dt \int_0^\infty S_i(u)\cos(2\pi ut)du \tag{3.7}$$

Definition of Hilbert Transform defined as below;

$$S_{Hi}(t) = \frac{1}{\pi}\int_{-\infty}^{\infty} \frac{s(t')dt'}{t'-t} \tag{3.8}$$

or

$$S_{Hi}(t) = -\frac{1}{\pi} * s(t) \tag{3.9}$$

3.4.3 Connectivity Metrics

By using Hilbert transform complex and real values of time series are obtained. These values were calculated with arctangent of fraction of the imaginary and real values. The phase information for time series is obtained as:

$$\phi(t) = \arctan\frac{s_i(t)}{s_r(t)} \tag{3.10}$$

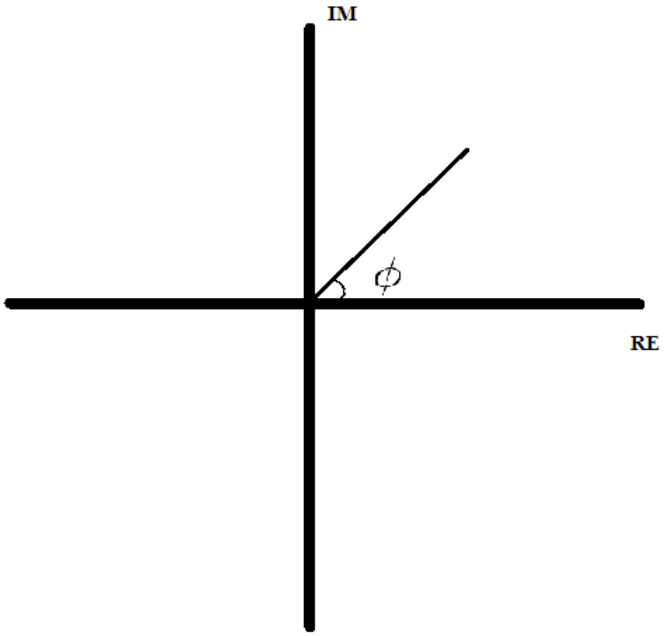

Figure 3.6 Imaginary and real axis. Analytical calculation of phase information.

Since the least square FIR filter is used, phase sequences' heads and tails are cut (500ms each) and 2500 millisecond parts of signals are obtained. After this cutting operation, a frequency dependent moving time-window is employed in a sliding mode. Length of time window was dependent to the lowest frequency of the band. This technique was first mentioned as "cycle-criterion" (CC) [49]. For calculation of window and sliding interval length these equations are used:

$$WindowLength = \frac{1}{LowestFilterFreq} * CC * SamplingFrequency \tag{3.11}$$

$$WindowSlide = \frac{WindowLength}{4} \tag{3.12}$$

With the formulas above; for each time window, PLV values are calculated and the graphs are obtained with the formula below:

$$PLV_{i,k}(t,f) = \frac{1}{N_{trials}} | \sum_{trial=1}^{N_{trials}} exp^{j(\phi_i^{trial}(t,f) - \phi_k^{trial}(t,f))} | \tag{3.13}$$

Graphs are calculated as weighted graphs. A threshold technique is used to

convert weighted graph into a binary graph. All the phase values are arranged in a descending order. Center of this time index is determined. Percent of this threshold value is multiplied with center index and the value found from the arranged phase values. Values below the threshold are equal to zero and those that are above the threshold are equal to one.

3.5 Graph Parameters and Types

Clustering coefficient (C) and path length (L) metrics are commonly used for characterizing structure of a graph. Clustering coefficient and path length values identify the network classification. In *regular networks*, a vertex is tied to almost all of the resting vertices with certain strength. Graphs of these networks possess average clustering coefficient and path length. Regular networks have high clustering coefficient and low path length values which means high resistive wires and low communication characteristics. In *random networks*, all edges are randomly obtained and have very low C and L. *Small-world networks* are the fraction of regular and random networks. Random networks have the same degree of probability distribution with that of regular networks. Similar to regular networks; those networks have closer clustering coefficient and small path length values. The networks which do not have the characteristics above are called *scale-free networks*.

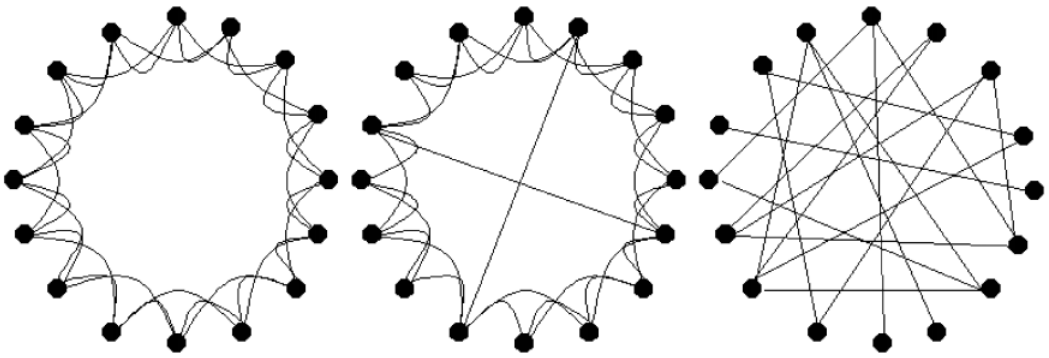

Figure 3.7 Types of networks. Regular network (left). Small-world network (center). Random network (right).

3.5.1 Clustering Coefficient

To define a clustering coefficient C_i, degree distribution k_i of a vertex i is the ratio of the existing edges e_i between its neighbors. So, degree is indicating the maximum possible neighbors which belong to that vertex. To calculate the clustering coefficient the following equation is used:

$$C_i = \frac{2e_i}{k_i(k_i - 1)} = \frac{\sum_{j,m} a_{i,j} a_{j,m} a_{m,i}}{(k_i - 1)} \tag{3.14}$$

Clustering coefficient varies between 0 and 1. To obtain a graph's global clustering structure, average clustering coefficient is calculated on N vertices. Average clustering coefficient is calculated as follows:

$$C = \langle c \rangle = \frac{1}{N} \sum_{i=1}^{N} c_i \tag{3.15}$$

In this study, clustering coefficient of the graph was found with an algorithm was discovered by Watts and Strogatz in 1998 [50].

3.5.2 Path Length

Second commonly used metric is the path length. The distance traveled between two vertices $d_{i,j}$ with the minimum number of edges from vertex i to j is called path length. Obtaining the integration of a graph in terms of easy communication is calculated by the average of those path lengths.

$$L = \frac{1}{N(N-1)} \sum_{i,j \epsilon N, i \neq j} d_{i,j} \tag{3.16}$$

3.5.3 Global Efficiency

When dealing with binary networks, weights of the graphs are converted to binary values by using specific threshold values. Values below the threshold are con-

sidered zero and the rest of them are considered as one. If a path of a network does not exist because of the threshold, L of this network is assumed to be infinite and therefore the efficiency of the network is zero. The calculation of the global efficiency of a network is as follows:

$$E_{global} = \frac{1}{N(N-1)} \sum_{i,j \epsilon N, i \neq j} \frac{1}{d_{i,j}} \tag{3.17}$$

3.5.4 Local Efficiency

When we consider a graph with pair wise nodes; to calculate average efficiencies of that local areas, local efficiency term is used:

$$E_{local} = \frac{1}{N} \sum_{i \epsilon N} E(G_i) \tag{3.18}$$

3.5.5 Edge and Node Betweenness Centrality

The number of shortest paths that runs through a vertex or edge has the centrality propery. Centrality is calculated by the ratio of all shortest paths between j and k that run through i ($n_{j,k}(i)$) is divided by all shortest paths between j and k ($n_{j,k}$). Betweenness centrality is calculated with the equation below:

$$b_i = \sum_{j,k \epsilon N, j \neq i} \frac{n_{j,k}(i)}{n_{j,k}} \tag{3.19}$$

3.6 Random Matrices and Their Efficiencies

For random matrices, randomization model of Maslov and Sneppen is used. This model satisfies the edge and vertex distribution of that created from the regular graph [51]. Implementation of this model, every connected node position changed with an unconnected node until it satisfies the requirements. Moreover, pair of connected nodes are selected randomly and selected nodes are rewired such that one node of first group

connected to another node of the second group. Only 100 node positions are changed, and operation is repeated for 100 times. For every iteration, clustering coefficients, path lengths and efficiencies are calculated to compute their averages.

4. RESULTS

After every experiment, mean reaction time, percentage of correct answers, fastest reaction time of correct answers, each trial status and it reaction times and click responses are recorded to a '.log' file. Preprocessed and segmented EEG data of subjects are imported into Matlab environment for further analysis. Only good segments for both manipulation and retention tasks are filtered by band pass filters with respect to the specific EEG frequencies (Table 4.1). Then, the filter outputs which are obtained from band pass filters, are decomposed into their imaginary and real samples with Hilbert transform. Angles of these values are calculated and specific parts are taken into account (Equation 3.10). Moving time windows were used for controlling the slowest synchronizing oscillation in order to avoid low temporal resolution. By using equation 3.13 PLV matrices are calculated. Binary adjacency matrices are obtained after threshold operation.

Table 4.1
Frequency bands and their lengths.

Band	**Frequency**	**Length of the filter**
Theta	4-8 Hz	749 Samples
Lower Alpha	8-10 Hz	375 Samples
Upper Alpha	10-13 Hz	299 Samples
Beta	13-30 Hz	229 Samples
Gamma	30-45 Hz	99 Samples

For each threshold value of each subject, local and global efficiencies are calculated with respect to the moving time windows and divided into equally distributed random matrices for normalizing global and local measure values to obtain small-world like characteristics. To determine significance meaning between manipulation and retention task groups, paired t-test is applied to global and local efficiencies for each threshold level. t-test decides whether difference for manipulation and retention group is zero or not. Paired t-test is used for controlled experimental studies to indicate how

they respond under various conditions. Manipulation and retention tasks provide the states for paired t-test. For each paired t-test probability values, false discovery rate (FDR) is calculated. FDR is a statistical tool which is used in multiple hypotheses testing to correct the multiple comparisons. FDR controls the expected proportion of incorrectly rejected null hypotheses. At the end of the paired t-test and FDR, most significant time windows are obtained, and those with mean significant differences are results of t-test.

Additionally, betweenness centrality is calculated for both edge and node centrality. Moving windows are summed up and combined into two time periods. Paired Wilcoxon sign rank test is applied for centrality metrics. This test checks wheather two series are coming from same population or indipendent. FDR results of this test are calculated and most significant nodes and edges are obtained. At the end, most significant edges and nodes of FDR and mean differences of significant results that come from paired Wilcoxon sign rank test are taken into account.

Mean values of local and global efficiency measures are plotted due to different threshold levels. Test statistic values of manipulation and retention differences are visualized over a rectangular scheme and most significant parts are marked with respect to thresholds and moving time windows. Node betweenness centrality measures of manipulation and retention tasks, and their differences are topologically plotted and most significant nodes are marked. In addition, statistically most significant edge centrality measures are placed on a brain electrode model, to show which parts of the brain and which frequency bands are related within working memory tasks through BrainNetVis software.

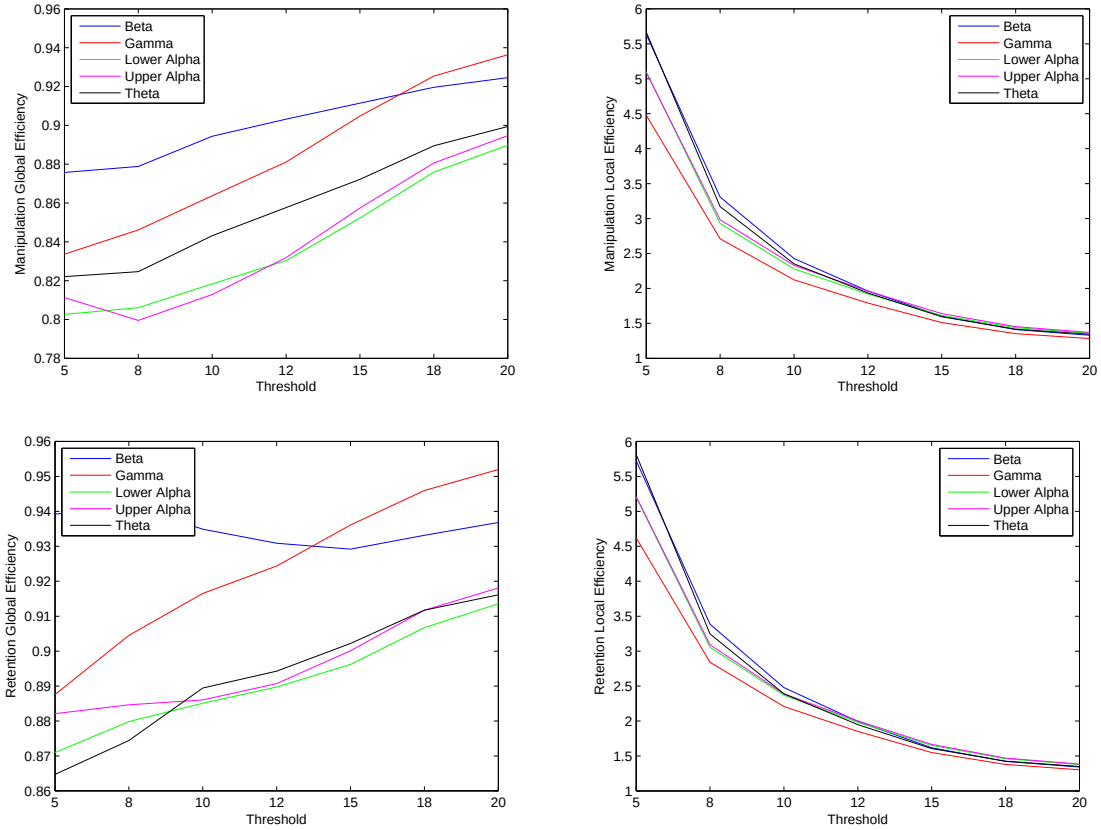

Figure 4.1 Average global and local efficiency variations over different thresholds for retention and manipulation tasks.

When the threshold values start to increase, the number of connected nodes decrease. Thus, the rise of normalized global efficiency values have proven the theory of small-world phenomena whereas the curve of small-world efficiency values stay between regular and random networks. In this sense, as the number of connected nodes in network decreases, efficiency of network converges to one. ($E_{Small-World} = \frac{E_{Regular}}{E_{Random}}$)

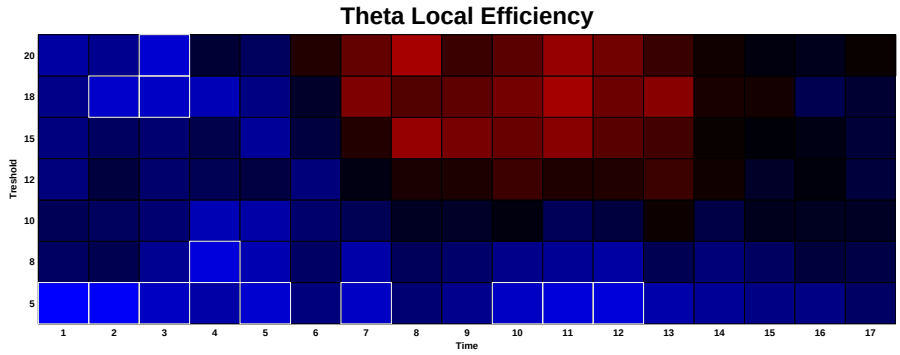

Figure 4.2 Local efficiency differences for different thresholds and windows for theta band.

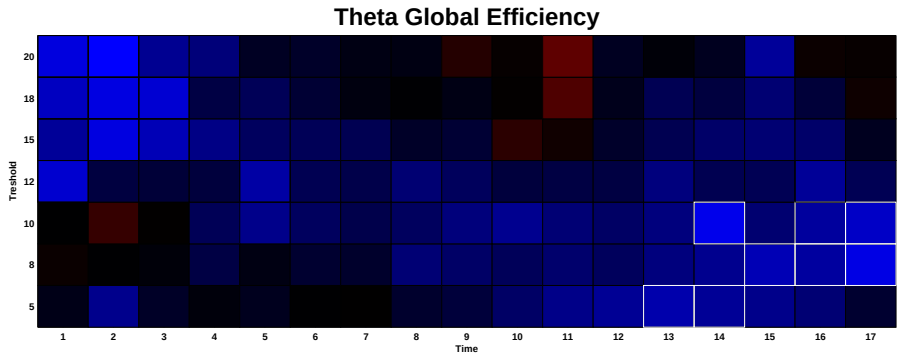

Figure 4.3 Global efficiency differences for different thresholds and windows for theta band.

To find the relationship between frequency dependent time windows and global efficiency for specific thresholds, mean differences between manipulation and retention are visualized. Negative values of manipulation-retention difference are marked with blue color for negative and red for positive.

Initially, local efficiency values are higher in retention task than manipulation. For the mid term, efficiency values for manipulation becomes more dominant for higher level of thresholds. Statistically, differences between manipulation and retention values are getting smaller for the final time windows. Significant differences in efficiency values are observed at lower threshold values (Figure 4.2).

A negative global efficiency difference in theta band is statistically singnificant towards the end of the decoding process. (Figure 4.3).

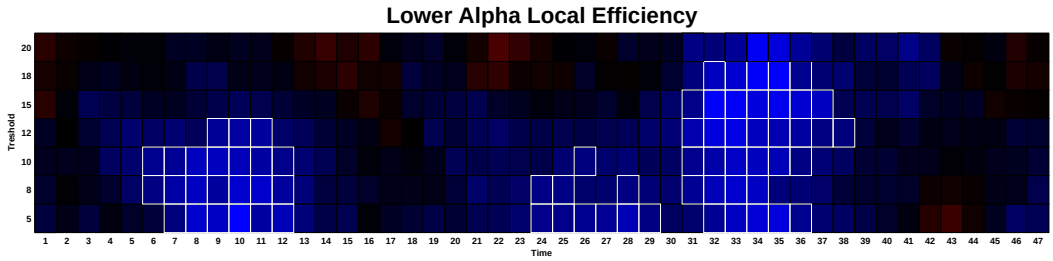

Figure 4.4 Local efficiency differences for different thresholds and windows for lower alpha band.

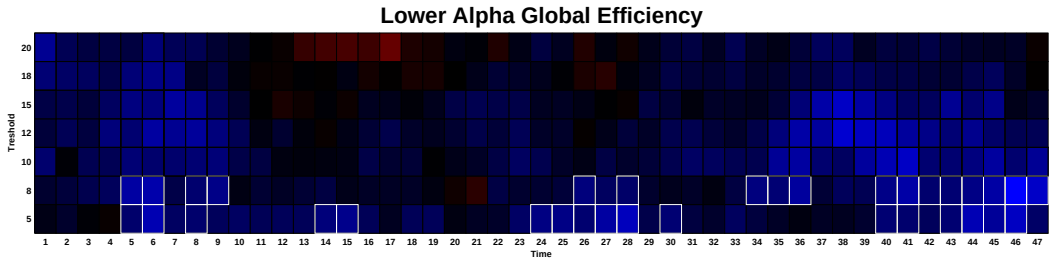

Figure 4.5 Global efficiency differences for different thresholds and windows for lower alpha band.

Statistical differences at the middle of the first time period and beginning of the second time period show significance retention dominance. When the number of connected nodes decreases, the mean local efficiency values decreases (Figure 4.4).

Manipulation-retention difference values are negatively signed at lower threshold levels (Figure 4.5).

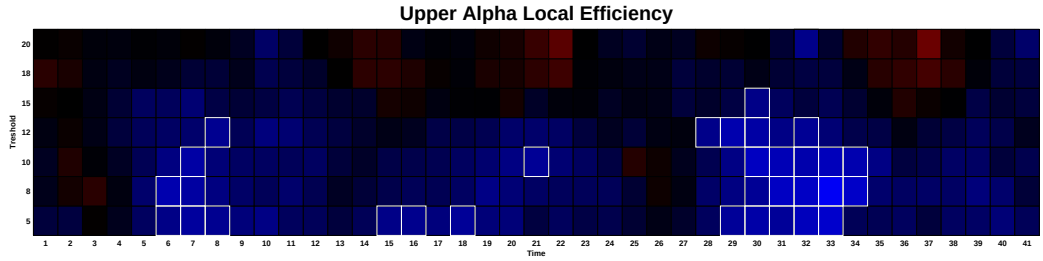

Figure 4.6 Local efficiency differences for different thresholds and windows for upper alpha band.

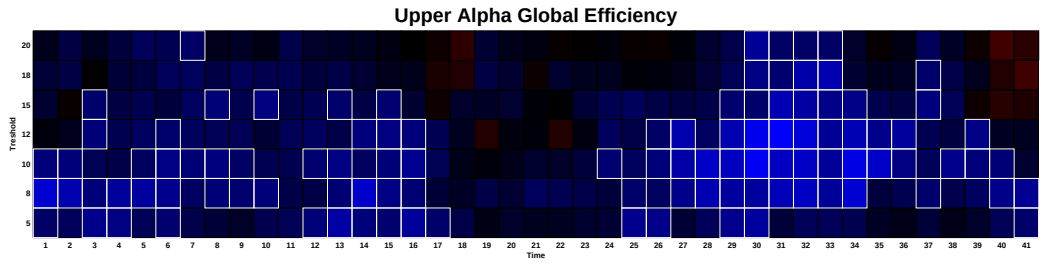

Figure 4.7 Global efficiency differences for different thresholds and windows for upper alpha band.

When the network is more connected, local efficiency values of retention task is getting more significant. Since the number of connected nodes decrease, manipulation becomes more dominant than retention. However, statistically significant differences are generally located at the first and the last time windows as threshold values are lowered (Figure 4.6).

Retention dominance is observes in the eighth and tenth threshold windows (Figure 4.7).

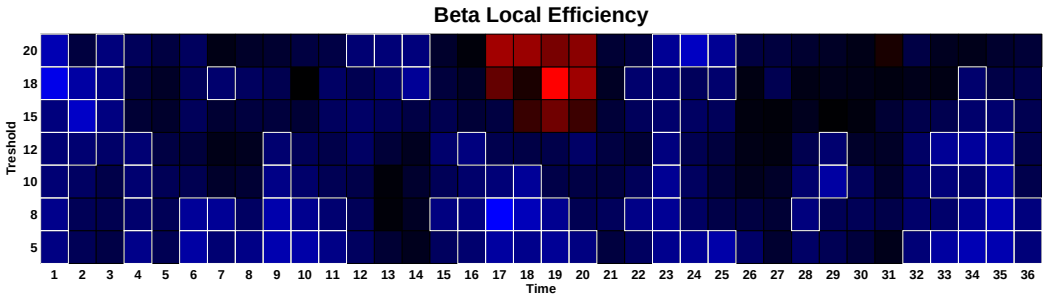

Figure 4.8 Local efficiency differences for different thresholds and windows for beta band.

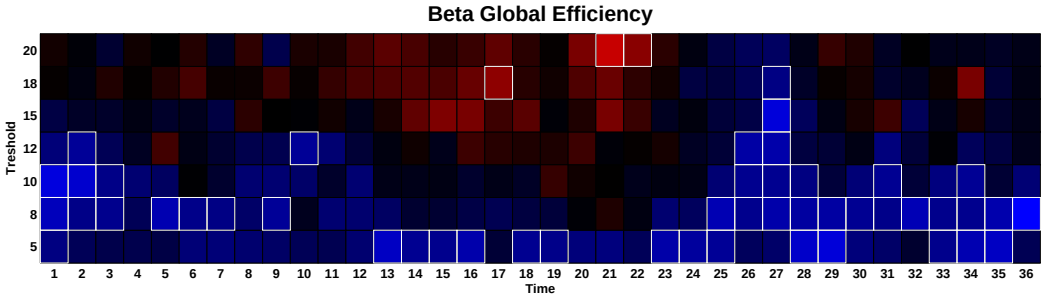

Figure 4.9 Global efficiency differences for different thresholds and windows for beta band.

Manipulation is more dominant at higher threshold values of the mid time windows whereas other parts indicate retention dominance. (Figure 4.8). Difference is positively signed at higher threshold levels. Statistically significant regions are located at lower threshold levels (Figure 4.9).

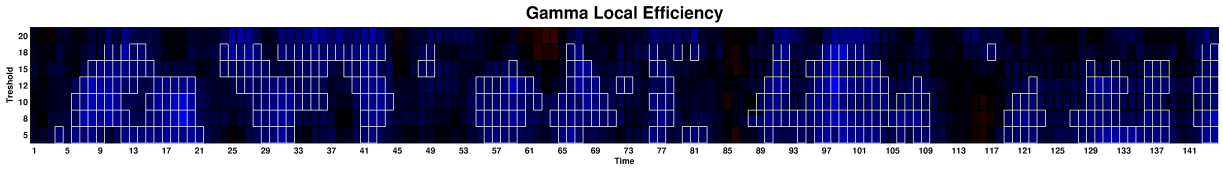

Figure 4.10 Local efficiency differences for different thresholds and windows for gamma band.

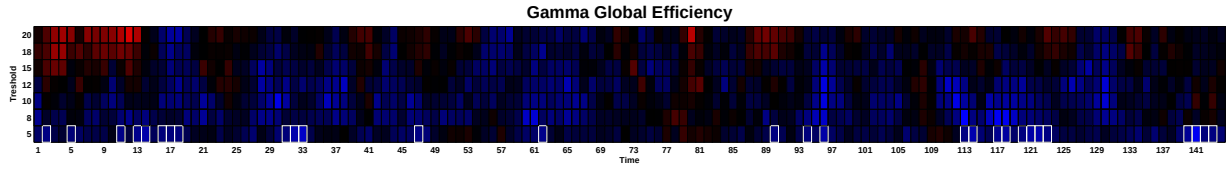

Figure 4.11 Global efficiency differences for different thresholds and windows for gamma band.

While the number of connected nodes decrease with higher level of thresholds, the number of statistically significant regions decrease (Figure 4.10).

Significant global structure of gamma band takes part with the lowest threshold level. Manipulation is more dominant with the increased number of disconnected nodes and is not showing a significant behavior. However, the rest of window show that the retention task is more dominant (Figure 4.11).

Time windows are summed up to obtain only two time windows. First window stands for first portion of manipulation/retention time and the second window stands for second portion. Nodes on parietal lobe and occipital lobe exhibit hub property for both manipulation and retention. Centrality values on left parietal lobe and left occipital lobe with the retention task is higher. Significant nodes of manipulation and retention difference is randomly distributed (Figure 4.12). At the second time period, right parietal lobe shows node property whereas retention task shows left parietal lobe. Left hemisphere indicates statistical significance (Figure 4.13).

For the first time period, all parietal and left hemisphere of frontal lobe show hub property for both tasks. Significant nodes are distributed over frontal and parietal lobe (Figure 4.14). Left parietal lobe centrality value on manipulation task is higher than retention task. Significant nodes of difference are distributed over frontal lobe (Figure 4.15).

Hub property is distributed over the scalp, not at occipital lobe but in parietal lobe. Significant nodes are condensed on parietal and frontal lobes (Figure 4.16). Centrality property is higher at retention task over the left parietal lobe. Significant nodes are distributed all over the scalp especially on parietal lobe (Figure 4.17).

For retention task, nodes at right and left hemisphere of scalp are in the form of a hub. However, lack of significant results show this hypothesis is not correct (Figure 4.18). Hub property of retention task is more advanced. Nodes at parietal and occipital region show significance (Figure 4.19).

Parietal lobe shows node property on retention task. Most of the nodes at difference are statistically significant over frontal and occipital regions (Figure 4.20). Only a small portion of parietal lobe shows hub property, especially on the right hemisphere. Significant nodes are distributed over all regions (Figure 4.21).

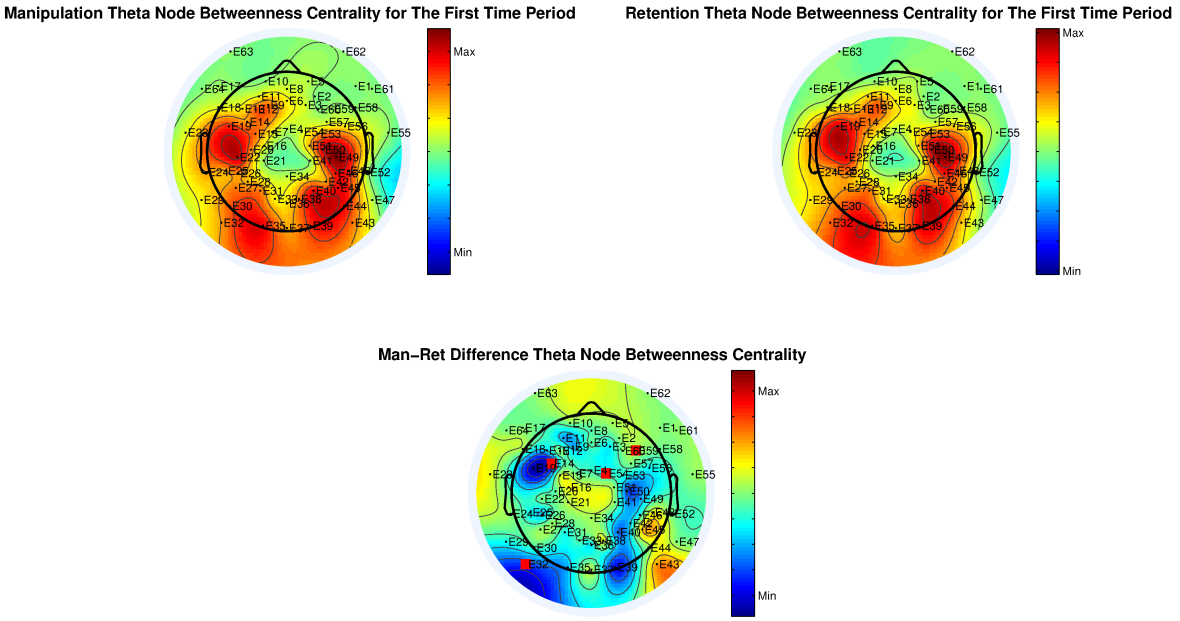

Figure 4.12 Theta band node betweenness centrality and their difference topology for manipulation and retention tasks of first time period.

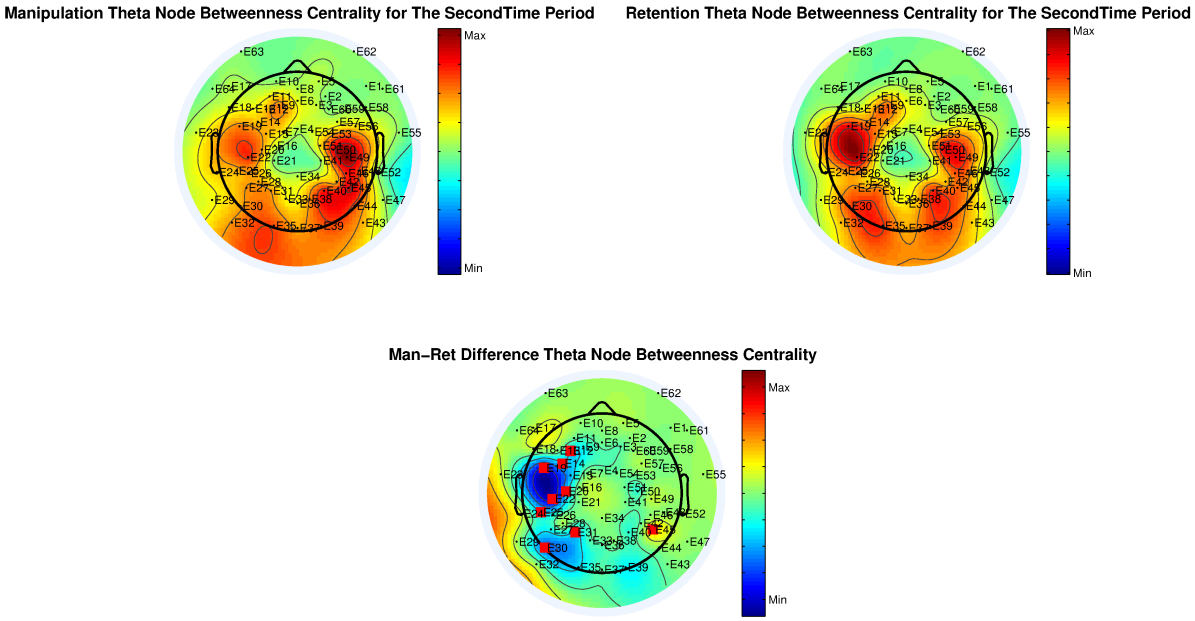

Figure 4.13 Theta band node betweenness centrality and their difference topology for manipulation and retention tasks of second time period.

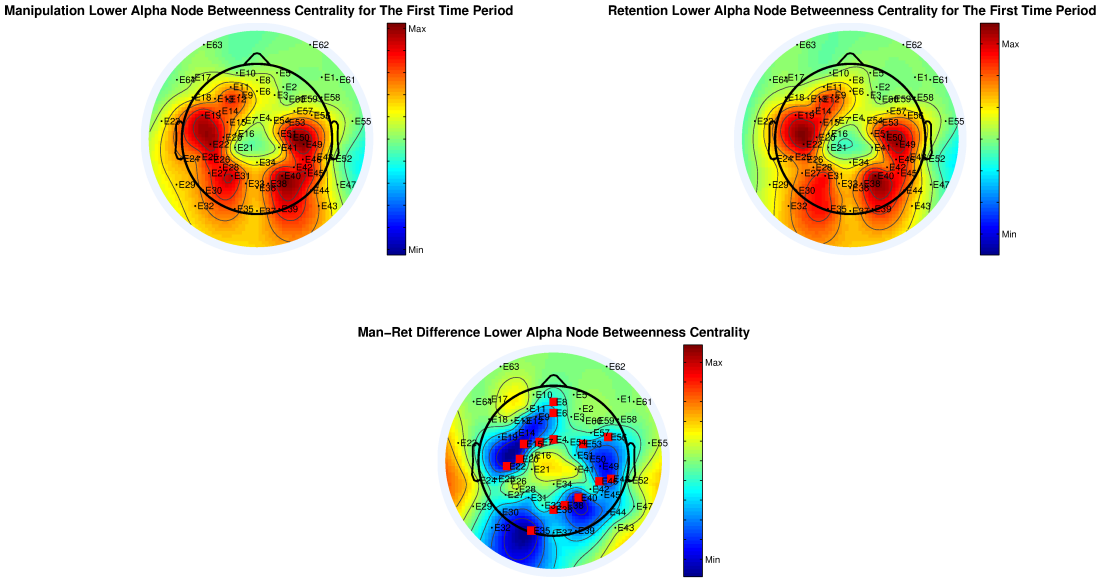

Figure 4.14 Lower alpha band node betweenness centrality and their difference topology for manipulation and retention tasks of first time period.

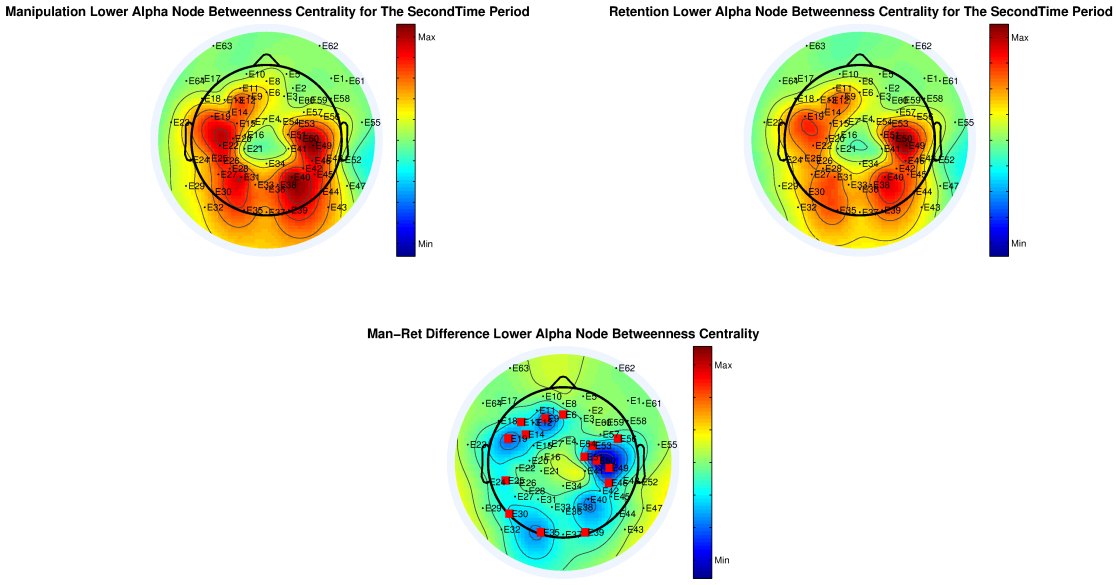

Figure 4.15 Lower alpha band node betweenness centrality and their difference topology for manipulation and retention tasks of second time period.

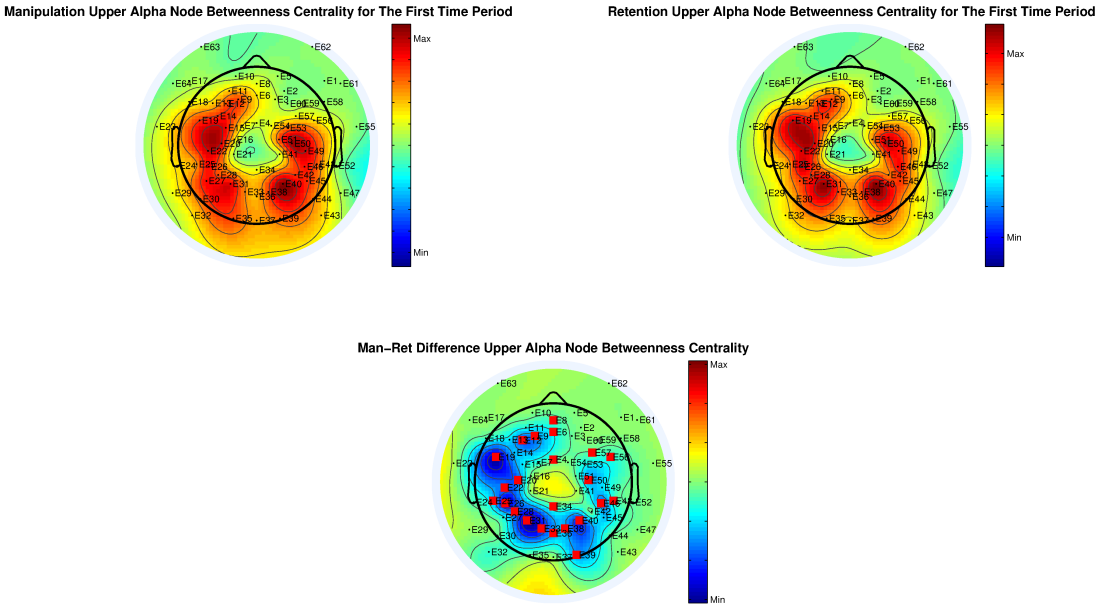

Figure 4.16 Upper alpha band node betweenness centrality and their difference topology for manipulation and retention tasks of first time period.

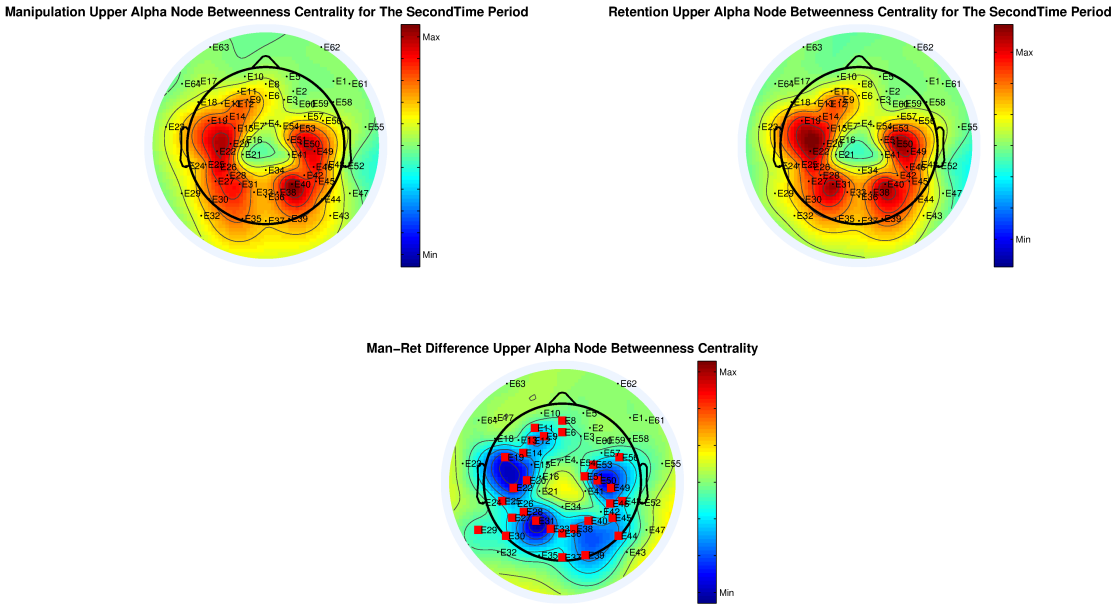

Figure 4.17 Upper alpha band node betweenness centrality and their difference topology for manipulation and retention tasks of second time period.

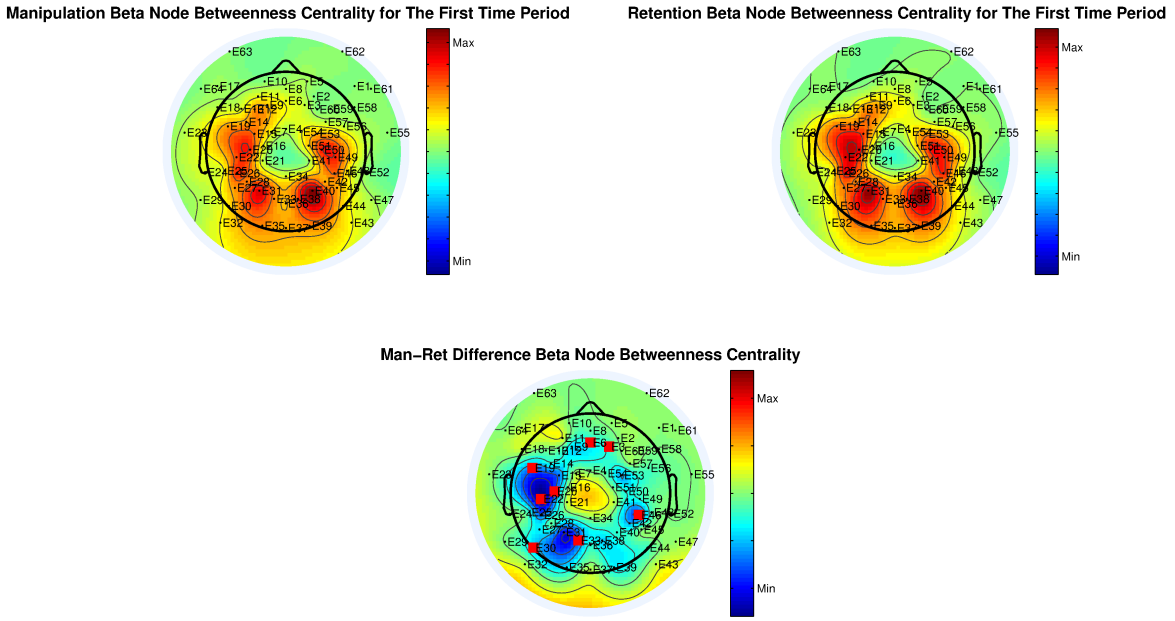

Figure 4.18 Beta band node betweenness centrality and their difference topology for manipulation and retention tasks of first time period.

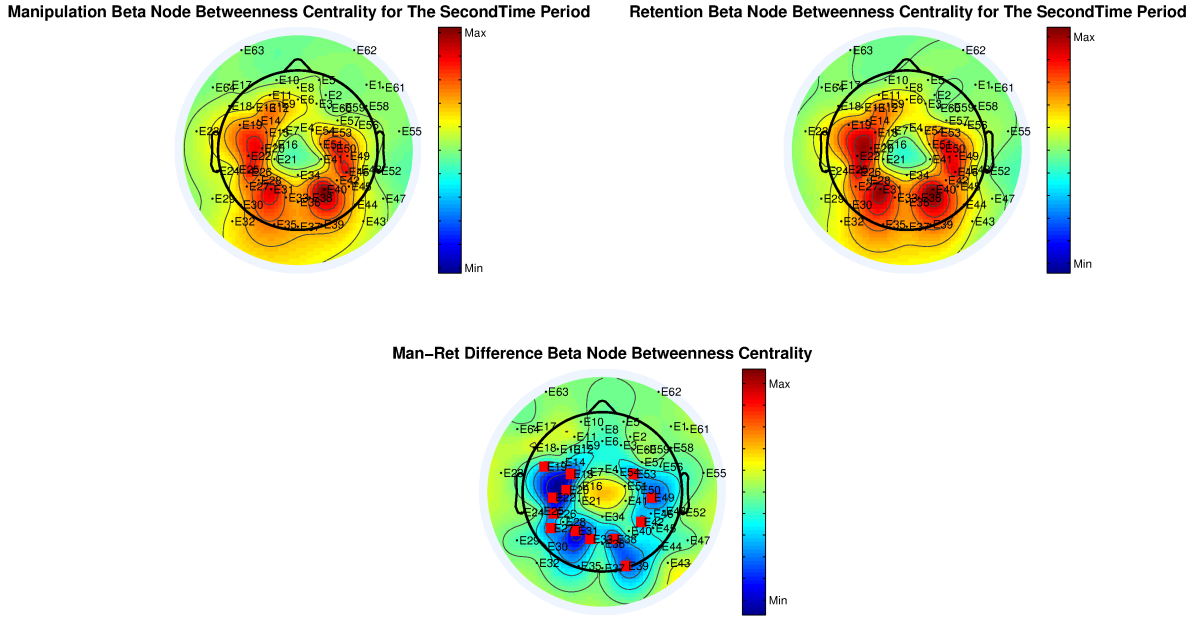

Figure 4.19 Beta band node betweenness centrality and their difference topology for manipulation and retention tasks of second time period.

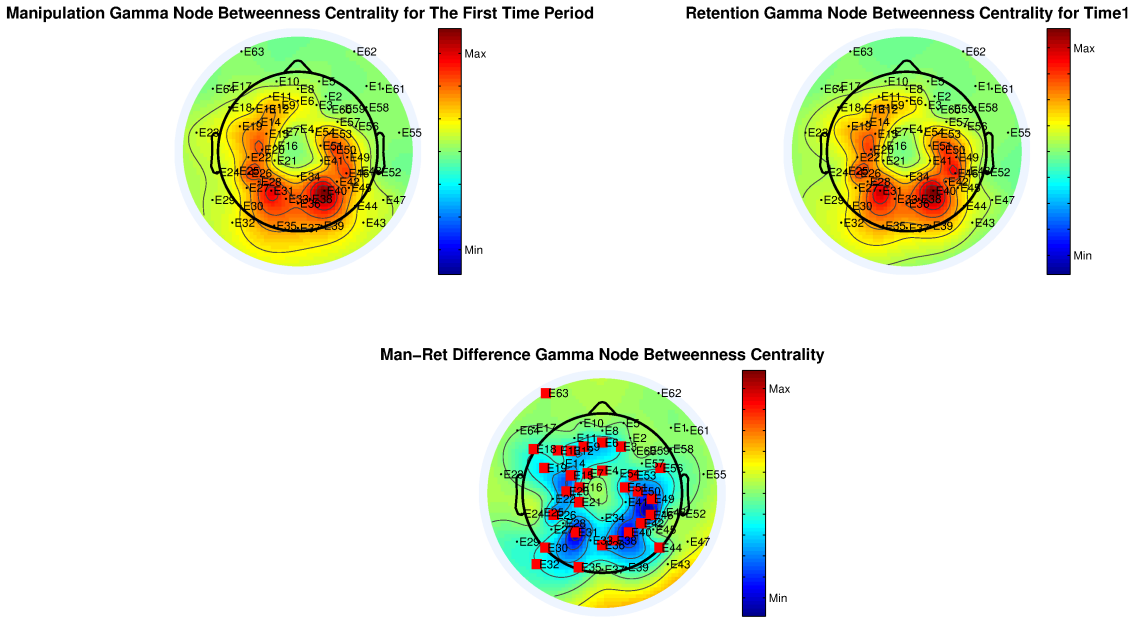

Figure 4.20 Gamma band node betweenness centrality and their difference topology for manipulation and retention tasks of first time period.

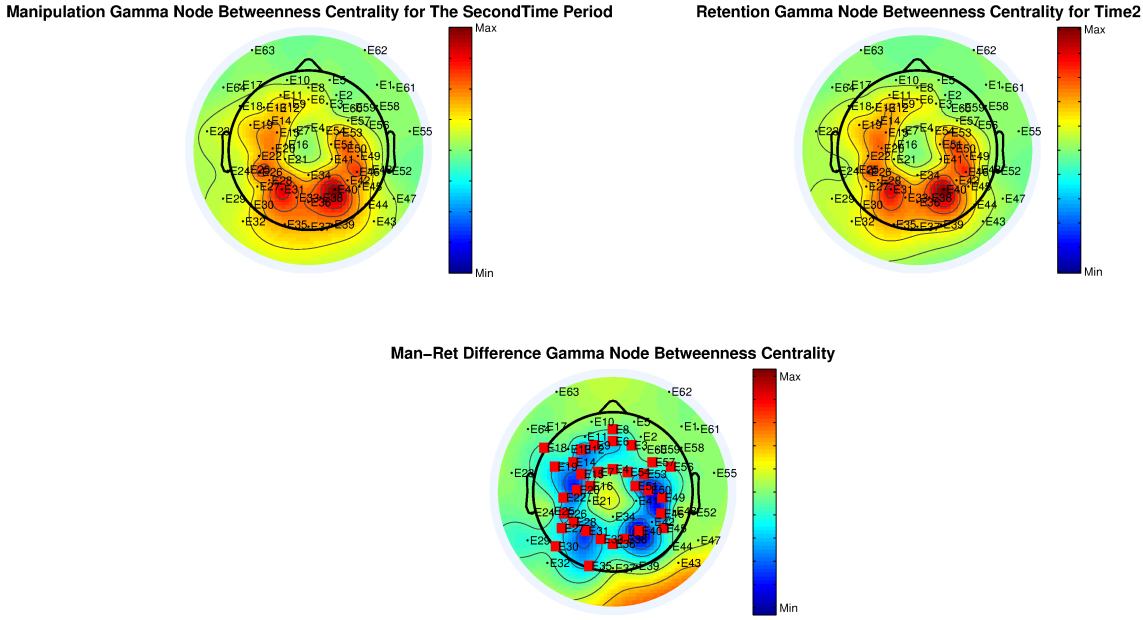

Figure 4.21 Gamma band node betweenness centrality and their difference topology for manipulation and retention tasks of second time period.

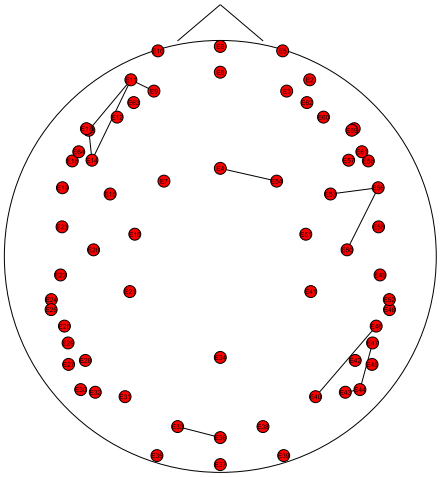

Figure 4.22 Theta edge betweenness centrality for time one.

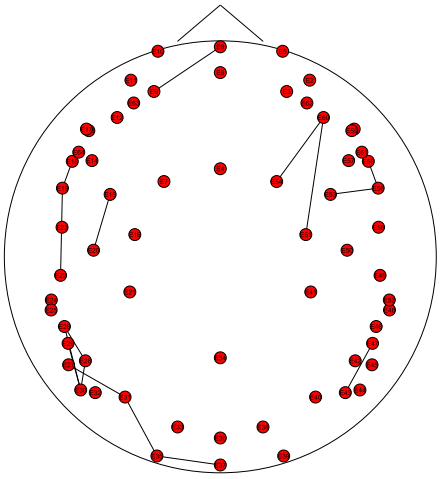

Figure 4.23 Theta edge betweenness centrality for time two.

FDR of the edge centrality values is between neighbor nodes. There is no intensive communication observed at the theta band.

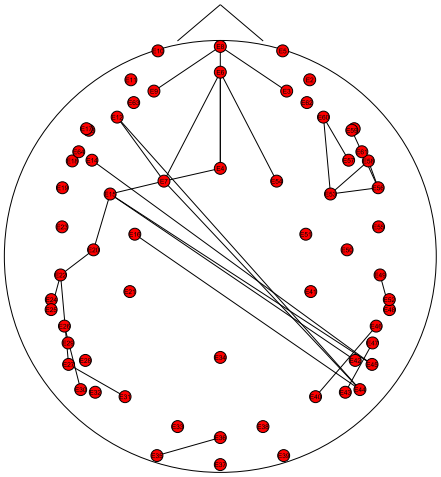

Figure 4.24 Lower Alpha edge betweenness centrality for time one.

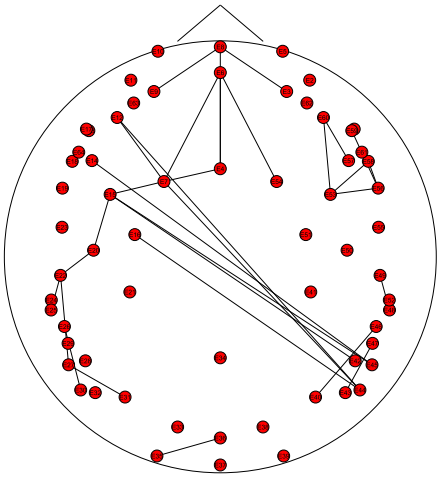

Figure 4.25 Lower Alpha edge betweenness centrality for time two.

For the first time period, upper alpha activity is more complicated than the second one. Information transfer flows from right parietal lobe to the left frontal lobes. Working memory is the combination of retention and execution. These result imply that, brain first executes at the frontal lobe then stores at the parietal lobe.

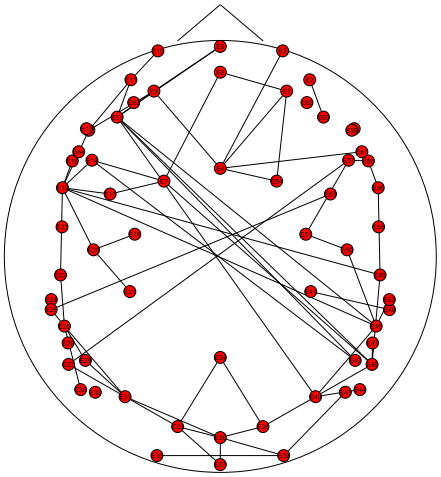

Figure 4.26 Upper Alpha edge betweenness centrality for time one.

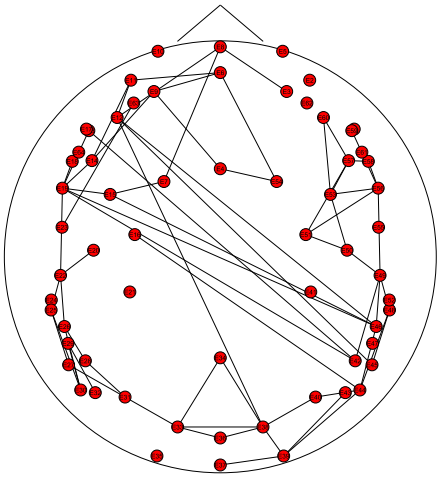

Figure 4.27 Upper Alpha edge betweenness centrality for time two.

At the upper alpha centrality relation, lower alpha like relation can be easily observed. However, for the first time period left frontal right parietal relationship is not explicable yet.

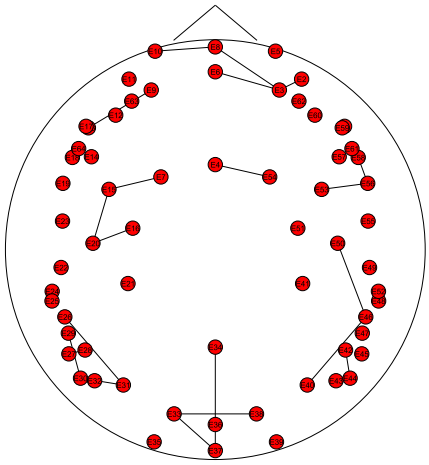

Figure 4.28 Beta edge betweenness centrality for time one.

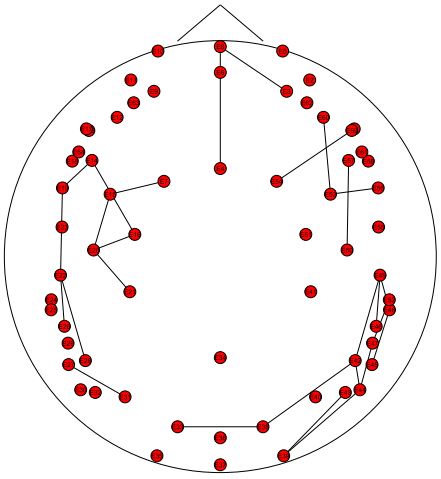

Figure 4.29 Beta edge betweenness centrality for time two.

In beta band, there is no observable evidence. Figure 4.28 and 4.29 show, the local connections are observed.

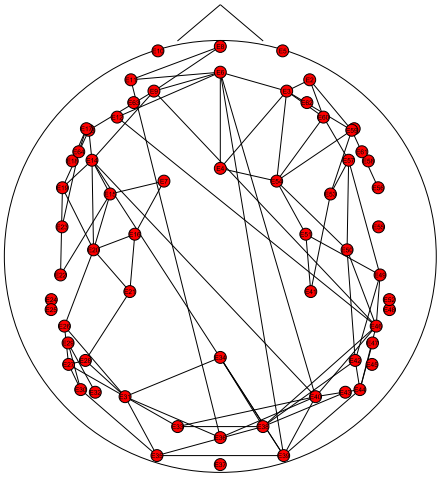

Figure 4.30 Gamma edge betweenness centrality for time one.

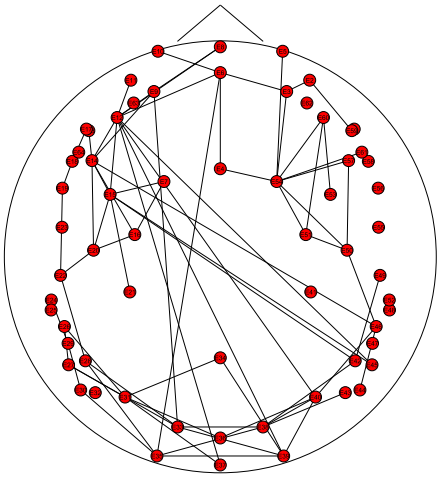

Figure 4.31 Gamma edge betweenness centrality for time two.

Local and global communication are shown in Figure 4.30 and 4.31. Like alpha bands, gamma has the communication links from the left frontal lobe to the right parietal lobe. Also small local connections at occipital lobe and left temporal lobe are expressed.

5. DISCUSSION

5.1 Global and Local Efficiency

Figure 4.1 shows the difference of random and regular efficiencies. Random networks have higher global efficiency than the regular ones [52]. ($E_{Small-World} = \frac{E_{Regular}}{E_{Random}}$)

Local efficiency of the regular graphs is higher than the random graphs (Figure 4.1). Brain had local efficiency greater than random networks. Achar et al. indicates same results and brain networks are low cost to medium cost networks [52]. High efficiency of parallel information is proportional transfer achieved with low cost of wiring.

5.2 Statistical Analysis of Efficiencies Over Time Windows and Thresholds

For all bands and time windows, statistical value of manipulation is greater than retention in an efficient manner. A property observed at the significant regions that manipulation-retention difference is maximum. Furthermore, significance of upper alpha global efficiency and gamma local efficiency is slightly obvious. However, for upper alpha local efficiency and gamma global efficiency is poor. Gamma has high frequency and its wavelength can be considered low [53, 54].

5.3 Node Centrality

Alpha activity of brain is associated with visual attention [55, 56]. According to our data, activity of alpha is travels through left frontal lobe to left parietal lobe.

So that, attention is starts at parietal lobe and executed at frontal lobe.

Theta activity is related between long time memory and short term memory. Less reflection is observed at theta band. Activity of theta started at occipital lobe to right parietal lobe. Recent studies suggested that theta activity is correlates with central executive functions such as working memory tasks [57]. Theta activity is correlated with encoding new information.

5.4 Edge Centrality

At lower alpha frequency edge centrality is between left frontal and left parietal. Attention starts at parietal lobe and executed at frontal lobe where this edge is the bridge of these regions in terms of communication. Same edge connections are transmitting routed information pathways. Short-range nodes are also communicating at upper alpha band. Upper alpha hubs can be attributed to visual attention [56]. A complex communication structure is operating at gamma band. Rather than long range connections short range connections are dense. However, Micheloyannis et al. suggested that theta band hubs are located in prefrontal region and related to working memory. Our data indicated nothing with the theta band [58].

6. CONCLUSION AND FUTURE WORK

The graph theoretical approach is one of the efficient mathematical tools to solve and analysis the various types of network. Whereas the brain is a complex structure, graph theoretical method fits the requirement of analysis of these kind of networks. In neuroscientific applications, graph theory has proven its success in previous studies which pioneered us to use specific metrics of graph theory in our thesis study.

Also graph theory is a common tool which investigates various networks in physics, social sciences and biology. In a neuroscientific point of view, graph was used in both neural and brain networks. Since the graph theory has rich parameter content, this study can be improved with the help of different metrics. Furthermore, most of the networks in the nature carry the small-world characteristics; applications in other sciences which have the same property can be applied to the brain networks. Moreover, our data collecting points are over the scalp. For future works, rather than using scalp data this study can be improved with source localization and clustering techniques.

REFERENCES

1. E. Niedermeyer, L. S., *Electroencephalography*, Wilkins, 1999.
2. Berger, H., "Über das Elektrenkephalogramm des Menschen," *Archiv für Psychiatrie und Nervenkrankheiten*, Vol. 87, pp. 527–570, Dec. 1929.
3. Caton, R., "Electrical currents of the brain," *British Medical Journal*, Vol. 87, pp. 278–282, Oct. 1875.
4. Buzsáki, G., "Theta Oscillations in the Hippocampus," *Neuron*, Vol. 33, pp. 325–340, Jan. 2002.
5. Tesche, C. D., and J. Karhu, "Theta oscillations index human hippocampal activation during a working memory task.," *Proceedings of the National Academy of Sciences of the United States of America*, Vol. 97, pp. 919–24, Jan. 2000.
6. Buzsáki, G., and A. Draguhn, "Neuronal oscillations in cortical networks.," *Science (New York, N.Y.)*, Vol. 304, pp. 1926–9, June 2004.
7. Daunizeau, J., O. David, and K. E. Stephan, "Dynamic causal modelling: A critical review of the biophysical and statistical foundations.," *NeuroImage*, pp. 1–11, Dec. 2009.
8. Bullmore, E., and O. Sporns, "Complex brain networks: graph theoretical analysis of structural and functional systems.," *Nature reviews. Neuroscience*, Vol. 10, pp. 186–98, Mar. 2009.
9. Lee, L., L. Harrison, and Mechelli, "A report of the functional connectivity workshop," *Neuroimage*, Vol. 19, pp. 457–465, 2002.
10. Amaral, L. a. N., and J. M. Ottino, "Complex networks," *The European Physical Journal B - Condensed Matter*, Vol. 38, pp. 147–162, Mar. 2004.
11. White, J., G., E. Southgate, N. Thompson, J., and S. Brenner, "The structure of the nervous system of the nematode," *C.Elegans, Phil.Trans.R.Soc.London*, Vol. 314, pp. 1–340, 1986.
12. Pachou, E., M. Vourkas, P. Simos, D. Smit, C. JStam, V. Tsirka, and S. Micheloyannis, "Working memory in schizophrenia: an EEG study using power spectrum and coherence analysis to estimate cortical activation and network behavior," *Brain Topography*, Vol. 21, pp. 128–137, 2008.
13. Rubinov, M., A. Knock S., J. Stam C, S. Micheloyannis, W. F. Harris, A., M. Williams L., and M. Breakspear, "Small-world properties of nonlinear brain activity in schizophrenia," *Human Brain Mapping*, Vol. 30, pp. 403–416, 2009.
14. Ponten, S., C., F. Bartolomei, and J. Stam, C., "Small-world networks and epilepsy: graph theoretical analysis of intracerebrally recorded mesial temporal lobe seizures," *Clinical Neurophsiology*, Vol. 118, pp. 918–927, 2007.
15. Sporns, O., "Network analysis,complexity,and brain-function," *Complexity*, Vol. 8, pp. 50–60, 2002.
16. Sporns, O., and G. M. Tononi, G.and Edelman, "Theoretical neuro anatomy:Relating anatomical and functional connectivity in graphs and cortical connection matrices," *Cerebral Cortex*, Vol. 10, pp. 127–141, 2000.

17. Cao, C., and S. Slobounov, "Alteration of cortical functional connectivity as a result of traumatic brain injury revealed by graph theory, ICA, and sLORETA analyses of EEG signals.," *IEEE transactions on neural systems and rehabilitation engineering : a publication of the IEEE Engineering in Medicine and Biology Society*, Vol. 18, pp. 11–9, Feb. 2010.

18. Jacobs, J., G. Hwang, and T. Curran, "EEG oscillations and recognition memory: Theta correlates of memory retrieval and decision making," *NeuroImage*, Vol. 32, pp. 978–987, 2006.

19. Euler, L., "Solutio problematis ad geometriam situs pertinentis," *Commentarii Academiae Scientiarum Imperialis Petropolitanae*, Vol. 8, pp. 128–140, 1736.

20. May, K. O., "The Origin of the Four-Color Conjecture," *Chichago Journals*, Vol. 56, pp. 346–348, 1965.

21. Klimesch, W., P. Sauseng, and S. Hanslmayr, "EEG alpha oscillations: the inhibition-timing hypothesis," *Brain research reviews*, Vol. 53, no. 1, pp. 63–88, 2007.

22. Milgram, S., "The small world problem," *Psychology today*, Vol. 2, no. 1, pp. 60–67, 1967.

23. Stam, C., W. Haan, and A. Daffertshofer, "Graph theoretical analysis of magnetoencephalographic functional connectivity in Alzheimer's disease," *Brain*, Vol. 132, pp. 213–224, 2009.

24. Sporns, O., and C. Honey, "Small worlds inside big brains," *Proceedings of the National Academy of Sciences*, Vol. 103, no. 51, p. 19219, 2006.

25. Sporns, O., G. Tononi, and R. Kï¿½tter, "The human connectome: A structural description of the human brain," *PLoS Computational Biology*, Vol. 1, p. e42, 09 2005.

26. He, Y., J. Chen, Z., and C. Evans, A., "Small-world anatomical networks in the human brain revealed by cortical thickness from MRI," *Cerebral Cortex*, Vol. 17, pp. 2407–2419, 2007.

27. Scannell, J., W., "The connectional organization of the cortico-thalamic system of the cat," *Cerebral Cortex*, Vol. 9, pp. 277–299, 1999.

28. Wang, J., L. Wang, Y. Zang, H. Yang, H. Tang, Q. Gong, Z. Chen, C. Zhu, and Y. He, "Neurophysiological architecture of functional magnetic resonance images of human brain," *Human Brain Mapping*, Vol. 15, pp. 1332–1342, 2005.

29. Babiloni, F., F. Cincotti, C. Babiloni, F. Carducci, D. Mattia, L. Astolfi, A. Basilicso, P. Rossini, L. Ding, Y. Ni, J. Cheng, K. Christine, J. Sweeney, and B. He, "Neurophysiological architecture of functional magnetic resonance images of human brain," *Neuroimage*, Vol. 24, pp. 118–131, 2005.

30. Wang, J., L. Wang, Y. Zang, H. Yang, H. Tang, Q. Gong, Z. Chen, C. Zhu, and Y. He, "Parcellation-dependent small-world brain functional networks: A resting-state fMRI study," *Human Brain Mapping*, Vol. 30, pp. 1511–1523, 2009.

31. Çiftçi, K., "Minimum Spanning Tree Reflects the Alterations of the Default Mode Network During Alzheimer's Disease," *Annals of Biomedical Engineering*, Vol. 39, pp. 1493–1504, 2011.

32. Fallani, F., V., L. Astolfi, F. Cincotti, D. Mattia, A. Tocci, S. Salinari, G. W. H. Marciani, M., A. Colosimo, and F. Babiloni, "Brain network analysis from high resolution EEG recordings by the application of theoretical graph indexes," *IEEE Transactions on Neural Systems and Rehabilitation Engineering*, Vol. 16, pp. 442–452, 2008.

33. Ganong, W., F., *Review of medical physiology*, Lange Medical Publications, 2001.

34. Squire L., R., E. Bloom F., K. McConnell S., L. Roberts J., C. Spitzer N., and J. Zigmond M., *Fundamental Neuroscience*, Academic Press, 2003.

35. Sayers, B., A., A. Beagley H., and R. Henshall W., "Mechanism of auditory evoked responses," *Nature*, Vol. 16, pp. 481–483, 1974.

36. Speckmann E., J., and E. Elger C., *Introduction to the neurophysiological basis of the EEG and DC potentials*, Williams and Wilkins, 1999.

37. Chang, H., T., *Handbook of Physiology*, American Physiological Society, 1984.

38. Chang, H., T., *Electroencephalography: General principles and clinical applications*, Churchill Livingstone, 2005.

39. Buzsáki, G., *Rythms of the brain*, Oxford University Press, 2006.

40. Varela, F., P. Lachaux, J., E. Rodriguez, and J. Martinerie, "The brainweb: phase synchronization and large-scale integration," *Nature Reviews Neuroscience*, Vol. 2, pp. 229–239, 2001.

41. Bassett, D. S., and E. Bullmore, "Small-world brain networks.," *The Neuroscientist : a review journal bringing neurobiology, neurology and psychiatry*, Vol. 12, pp. 512–23, Dec. 2006.

42. Stam, J., and C. Reijneveld, "Graph theoretical analysis of complex networks in the brain," *Nonlinear Biomedical Physics*, Vol. 1, pp. 1–19, 2007.

43. Freeman, L. C., "A set of measures of centrality based on betweenness," *Sociometry*, Vol. 40, pp. 35–41, 1977.

44. Girvan, M., and M. E. J. Newman, "Community structure in social and biological networks.," *Proceedings of the National Academy of Sciences of the United States of America*, Vol. 99, pp. 7821–6, June 2002.

45. Friston K., J., "Functional and effective connectivity in neuroimaging: a synthesis," *Humman Brain Mapping*, Vol. 2, pp. 56–78, 1994.

46. Sauseng, P., W. Klimesch, M. Doppelmayr, T. Pecherstorfer, R. Freunberger, and S. Hanslmayr, "EEG alpha synchronization and functional coupling during top-down processing in a working memory task.," *Human brain mapping*, Vol. 26, pp. 148–55, Oct. 2005.

47. Erdös, P., and A. Rényi, "On the random graphs," *Publicationes Mathematicae*, Vol. 6, pp. 290–297, 1959.

48. Haykin, S., *Communication Systems*, John Wiley, 1994.

49. Cohen, M. X., "Assessing transient cross-frequency coupling in EEG data.," *Journal of neuroscience methods*, Vol. 168, pp. 494–9, Mar. 2008.

50. Watts, D. J., and S. H. Strogatz, "Collective dynamics of 'small-world' networks.," *Nature*, Vol. 393, pp. 440–2, June 1998.

51. Maslov, S., and K. Sneppen, "Specificity and stability in topology of protein networks.," *Science (New York, N.Y.)*, Vol. 296, pp. 910–3, May 2002.

52. Achard, S., and E. Bullmore, "Efficiency and cost of economical brain functional networks.," *PLoS computational biology*, Vol. 3, p. e17, Feb. 2007.

53. Klimesch, W., "EEG alpha and theta oscillations reflect cognitive and memory performance: a review and analysis.," *Brain research. Brain research reviews*, Vol. 29, pp. 169–95, Apr. 1999.

54. Palva, S., and J. M. Palva, "New vistas for alpha-frequency band oscillations.," *Trends in neurosciences*, Vol. 30, pp. 150–8, Apr. 2007.

55. Stein, A. V., and J. Sarnthein, "Different frequencies for different scales of cortical integration: from local gamma to long range alpha/theta synchronization," *International Journal of Psychophysiology*, Vol. 38, no. 3, pp. 301 – 313, 2000.

56. Sauseng, P., W. Klimesch, W. Stadler, M. Schabus, M. Doppelmayr, S. Hanslmayr, R. Gruber, W., and N. Birbaumer, " A shift of visual spatial attention is selectively associated with human EEG alpha activity," *European Journal of Neuroscience*, Vol. 22, pp. 2917–2926, 2005.

57. Klimesch, W., R. Freunberger, P. Sauseng, and W. Gruber, "A short review of slow phase synchronization and memory : Evidence for control processes in different memory systems ?," *Review Literature And Arts Of The Americas*, Vol. 5, 2008.

58. S., M., V. Sakkalis, M. Vourkas, J. Stam, C., and S. P. G., "Neural networks involved in mathematical thinking: evidence from linear and non-linear analysis of electroencephalographic activity," *Neuroscience Letters*, Vol. 7, pp. 212–219, 2005.